DESIGN AND DEVELOPMENT OF REMOTE RAMAN SPECTROSCOPY SYSTEM FOR DETECTION OF HAZARDOUS COMPOUNDS

By

William Ortiz-Rivera

A dissertation submitted in partial fulfillment of the requirements for the degree of

DOCTOR OF PHILOSOPHY
in
Applied Chemistry

UNIVERSITY OF PUERTO RICO
MAYAGÜEZ CAMPUS
NOVEMBER 2012

Approved by:

_____	_____
Samuel P. Hernández-Rivera, PhD President, Graduate Committee	Date
_____	_____
Camen A. Vega, PhD Member Graduate Committee	Date
_____	_____
Nilka Rivera, PhD Member Graduate Committee	Date
_____	_____
Julio G. Briano-Peralta, PhD Member Graduate Committee	Date
_____	_____
Carmen Bellido, PhD Representative of Graduate Studies	Date
_____	_____
René S. Vieta, PhD Chairperson of the Department	Date

ABSTRACT

Remote Raman detection has become a powerful analytical technique for detection of hazardous compounds *in situ* and without sample preparation at distances away from the observation site. This study describes the design, assembly, testing and validation of Remote Raman Spectroscopy (RRS) systems intended for stand-off detection of hazardous chemicals such as explosives: TNT, PETN, RDX and TATP; chemical warfare agents simulants: dimethylmethylphosphonate, 2-chloroethyl ethyl sulfide and 2-(butylamino)-ethanethiol; and Toxic Industrial Compounds: benzene, chlorobenzene, toluene, carbon tetrachloride, cyclohexane and carbon disulfide.

The prototype systems consisted of a spectrometer equipped with a CCD detector (for CW measurements) and an I-CCD camera with time-gated electronics (for pulsed laser measurements), a reflecting telescope, fiber optic assemblies, single-line continuous wave (CW) laser sources (514.5, 488.0, 351.1 and 363.8 nm) and a frequency-doubled single frequency Nd:YAG 532 nm pulse laser (5 ns pulses at 10 Hz repetition rate). The telescope was coupled to the spectrograph using an optical fiber and notch filters were used to reject laser radiation and Rayleigh scattering. Two quartz convex lenses were used to collimate the light from the telescope from which the telescope-focusing eyepiece was removed, and direct it to the fiber optic assembly. The stand-off detection systems were tested employing the compounds mentioned at different remote distances (2 to 141 m) using several sampling approaches. Quantification and classification of explosives (TNT and PETN) hidden in non-explosives matrices (4-NBA and APAP) with similar chemical structures were achieved in powder mixtures by using chemometrics techniques.

RESUMEN

La detección remota empleando la espectroscopia Raman, se ha convertido en una poderosa técnica analítica útil en la detección remota de compuestos peligrosos *in situ* y sin preparación de muestras. En esta investigación se describe el diseño, ensamblaje, y prueba de un sistema de detección remota empleando espectroscopia Raman destinado para la detección a distancia de sustancias químicas peligrosas como explosivos:(TNT, PETN, RDX y TATP); simulantes de agentes químicos empleados en conflictos belicos: (dimetilmetilfosfonato, sulfuro de 2-cloroetilo, 2-(butiloamino)-etanotiol y compuestos industrial tóxicos: benceno, clorobenceno, tolueno, tetracloruro de carbono, ciclohexano y disulfuro de carbono. El sistema de detección consistió de un espectrómetro equipado con un detector CCD (para mediciones empleando laser de onda continua) y una cámara I-CCD (para mediciones con laser pulsado), un telescopio reflector, fibras ópticas, laser de onda continua (514.5, 488.0 nm) y la segunda armónica a 532 nm de un laser pulsado Nd:YAG (con un pulsos de 5 ns y una rapidez de repetición de 10 Hz). El telescopio se acopló a el espectrógrafo por medio de una fibra óptica, un filtro “notch”. El ocular del telescopio fue modificado por dos lentes biconvexos de cuarzo para hacer converger la señal Raman recogida por el telescopio y transmitida hacia la fibra. Nuestro sistema de detección remota se validó con los compuestos mencionados a diferentes distancias (2 a 141m) usando diferentes técnicas de muestreo. Se llevaron a cabo estudios de cuantificación y discriminación de explosivos (TNT y PETN) escondidos deliberadamente en matrices con estructura química parecida (4-NBA y APAP) empleando técnicas de quimiometría.

Dedication

To:

God

My wife Jenifier, my daughter Isabella Del Mar and my parents

ACKNOWLEDGMENTS

I would like to express my most sincere appreciation to all the people that in one way or another have contributed positively in the completion of this research. Sincerely, I thank the Almighty for giving me the wisdom, patience and above all perseverance to be able to overcome all obstacles and challenges in the wonderful world of science. I immensely thank my advisor Dr. Samuel P. Hernández for giving me the opportunity to do research under his guidance and supervision at the Center for Chemical Sensors Development, Department of Chemistry, University of Puerto Rico-Mayaguez. I also wish to share this acknowledgement with my partners from Dr. Hernández's laboratory, especially Dr. Leonardo C. Pacheco-Londoño for his valuable intellectual contribution to this research.

To my friends: Hilsamar, John, Eduardo, Jose, Pedro, Jorge, Nataly, Hector, Raymond, Carlos, Nelson, Guette and Manuel for all the pleasant and fun moments we shared during my stay in graduate school at UPRM.

Thanks to my graduate committee members, who help me with direction, suggestions and corrections in this research work, please receive all my thanks: Dr. Carmen Vega, Dr. Nilka Rivera and Dr. Julio Briano. Thanks to the Chemistry Department at UPR-Mayagüez: Professors and administrative personal. Thanks to Dr. Wilfredo Otaño for the opportunity to complete the internship requirement.

Sincerely, I would like to thank to my wife Jenifier and my little girl Isabella Del Mar for all unconditional support, patience and love in all situations of happiness and sadness.

Parts of the work presented in this contribution were supported by the U.S. Department of Defense, University Research Initiative- Multidisciplinary University Research Initiative

(URI)-MURI Program, under grant number DAAD19-02-1-0257. Support from the U.S. Department of Homeland Security under Award Number 2008- ST-061-ED0001 is also acknowledged.

TABLE OF CONTENTS

Table List

Figure List

1. INTRODUCTION

1.1 Motivation

During recent years, the world has suffered many terrorist attacks by use of explosives and chemical warfare agents, such as the attack in Madrid on March 11, 2004, where near-simultaneous coordinated attacks targeting commuter trains in Madrid was executed by Basque separatist militant group ETA. In London on July 7, 2005, several explosions in a bus and four subway stations occurred almost simultaneously during the rush hours of the morning. These events completely affected the entire buses and underground transportation network, casting shadows on the joy of Londoners, who had been recently selected as hosts for the 2012 Olympic Games. These and other terrible events have motivated many countries to focus their research toward the detection of explosives, hazardous liquids, and chemical agents that can be employed by terrorist organizations as threats against troops and/or civilians.

The anticipation of future attacks requires a wide array of detection systems for potential deployment scenarios [1, 2].

An explosive is described as a meta-stable agent before detonation. Actual detonation is characterized by extremely rapid reaction rates, measured in sub-milliseconds. Products of this detonation are gasses, heat and high pressures. Explosives can be classified by their performance and uses. Primary explosives also known as low explosives undergo very rapid transition from burning to detonation. These are capable of transmitting the detonation to less sensitive explosives. Detonation can occur by heat or shock. Examples of primary explosives are mercury fulminate and lead azide. Secondary explosives, also known as high explosives, cannot be detonated readily by heat or shock and they are less sensitive than primary explosives, so they need primary explosives to detonate them. Examples of secondary explosives are 2,4-

dinitrotoluene (DNT), 2,4,6-trinitrotoluene (TNT), and hexahydro-1,3,5-trinitro-1,3,5-triazine (RDX). TNT is one of the high explosives that has been used for military purposes since 1902.

Chemical Warfare Agents (CWA) most likely to be used as terrorist weapons, according to terrorism experts include nerve agents, blister agents, choking agents and blood agents. Nerve agents are a group of particularly toxic CWA [3, 4]. They were developed just before and during World War II and are chemically related to organophosphorus insecticides. The principal compounds in this group are: Tabun (GA), Sarin (GB), Soman (GD), and methylphosphonothioic acid (VX). Characterization of hydrolysis and or degradation products of CWA has been documented to provide still another capability to detect possible attacks to water systems [2, 3].

During the last few years, the topic of explosives detection has been an active research area. The need for security screening prompted a variety of schemes for detection of trace amounts of energetic materials [5]. Several techniques have been employed to detect and identify explosives, hazardous liquids and chemical warfare agents simulants including HPLC/MS, GC/MS, IMS, infrared spectroscopy, Raman spectroscopy, among others. Vibrational spectroscopy has the advantage that provides chemical information besides detection capabilities. Raman spectroscopy is a non-destructive and non-invasive technique that requires little sample treatment and has the potential for remote sensing.

There is a need for more sensitive and selective remote detection techniques for explosives operating at ambient conditions, *in situ* and in real-time scale. Therefore, standoff Raman spectroscopy (SRS) provides a method for identifying chemicals in a sample located meters from the excitation source. In fact, telescope based Raman spectroscopy detection methods have been reported for standoff detection of chemicals using both visible and UV laser

excitation [6–13]. This distance can vary from a few centimeters, for monitoring chemicals in a manufacturing process, to tens of meters when examining potentially dangerous samples such as explosives. SRS has been demonstrated and is used in several areas, including explosives detection, atmospheric analysis and detection of different organic and inorganic compounds.

1.2 Literature review

Several information collected and presented below describing the capability of Raman spectroscopy for development remote sensing technology based on Raman telescope for detection of hazardous compound and has been already published in several peer-review publications by the author and the mentor [14-16].

1.2.1 Raman Spectroscopy

1.2.2 Scattering of Light

Raman spectroscopy is a high resolution photonic technique that provides spectroscopic information that can be used to convey chemical and structural information about any organic and inorganic compounds in a few seconds to minutes. The Raman effect was originally observed in 1928 (Figure 1) by the physicist Chandrasakhar V. Raman. Sir C.V. Raman first observed the phenomenon using sunlight and was awarded the Nobel Prize in Physics for this discovery in 1930 [17, 18]. The Raman event occurs when a monochromatic light of frequency ν_o encounters a sample (gas, solid or liquid). When analyzing the light scattered by the sample, it is found that most of the scattered light presents the same frequency as the incident light (elastically scattered radiation). The light that keeps the same frequency ν_o that the incident light is known as elastic or Rayleigh scattering and provides no information on the composition of the

sample. A small fraction of the emerging light photons shows frequency shifts resulting from the interaction of light with matter (inelastically scattered radiation). Scattered light that presents different frequencies to that of the incident radiation is known as Raman scattering. The new frequencies $\nu_o + \nu_R$ and $\nu_o - \nu_R$ are Raman frequencies, which are characteristic of the nature and physical state of the sample and independent of the incident radiation.

Variations in the observed frequency in Raman scattering phenomenon, are equivalent to variations in energies. Ions and atoms chemically bonded to form molecules and crystalline networks are subjected to constant vibrational and rotational movement. These oscillations are observed at certain frequencies based on the masses of particles involved and the dynamic behavior of the bond that exist. Each of these vibrational and rotational movements of the molecule corresponds to a certain value of molecular energy. When the photon beam incident light, with energy ($h\nu_o$) much greater than the difference in energy between two vibrational (or rotational) levels of the molecule collides with the molecule, most of the photons pass by without interacting with the molecular system. However a small fraction are inelastically scattered (of the order of 1 scattered photon per 10^7 incident photons). This scattering can be interpreted as the following process: the incident photon leaves the molecule temporarily to a higher level of energy vibrational or rotational (virtual state) which is not an allowed or stationary state, which quickly decays to an allowed energy level emitting a photon. If scattered photon is the result of the photon-molecule interaction, its frequency differs of the incident frequency, this collision is termed inelastic. This means that there is a transfer of energy between the photon and the molecule, in this case two phenomena may occur: If the scattered photon has lower frequency than the incident one, there is a transfer of energy from photon to the molecule that after moving into a forbidden energy state, and returns to its allowed initial energy state, the photon is

scattered with frequency $\nu_o - \nu_m$ and Stokes Raman dispersion occurs. Another possible phenomenon occurs if the scattered photon has a higher frequency than the incident, there is a transfer of energy from the molecule to the photon. This means that initially before the collision occurred the molecule was not in its lowest vibrational state, but one of higher energy. After the collision takes place, the photon is scattered with a frequency $\nu_o + \nu_m$ and Raman anti-Stokes scattering occurs. At room temperature, according to the Maxwell-Boltzmann law of distribution of energy, 99% of the molecules are in the lowest possible vibrational state (ground vibrational state). Therefore, the probability of Raman Stokes scattering occurrence are greater than the Raman anti Stokes scattering. These processes are illustrated in Figure 1.

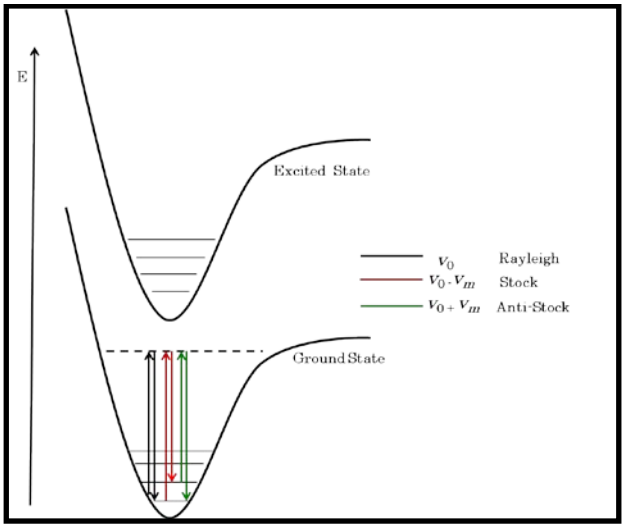

Figure 1. Energy diagram for Raman scattering representation.

1.2.3 Classical Theory of Raman Effect

As discussed above, an incident electromagnetic wave induces an electric dipole moment during the light-material interaction (Fig. 2). The strength of the induced dipole moment, P, is given by

$$\boldsymbol{P} = \alpha \boldsymbol{E} \quad \textbf{(1)}$$

The magnitude of the induced dipole moment ***P*** depends upon the amplitude of the light wave and the polarizability (α) of the molecule which is a measure of how readily the electrons are displaced in the field ***E*** of the light wave. The polarizability is a material property that depends on the molecular structure and nature of the bonds. For the incident electromagnetic wave, the magnitud of the electric field vector may be expressed as:

$$E = Eo \cos(2\pi \nu o t), \quad \textbf{(2)}$$

where ν_o is the frequency (Hz) of the incident EM ($\nu_o = c/\lambda$). Substituting Eq. (2) into (1) yields the time-dependent induced dipole moment,

$$P = \alpha\, Eo \cos(2\pi \nu o t). \quad \textbf{(3)}$$

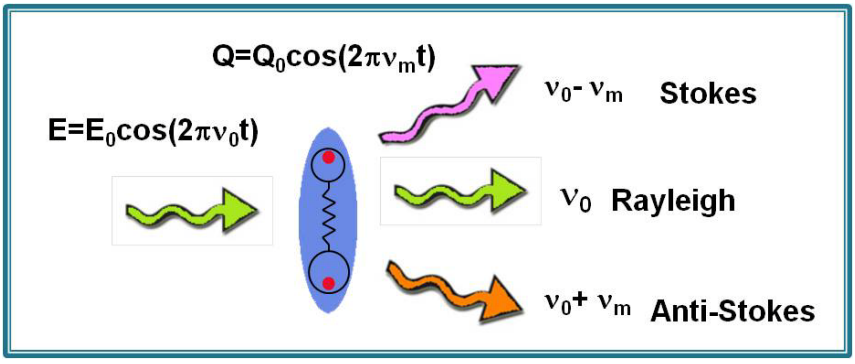

Figure 2. Interaction of a light wave with a diatomic molecule.

Because the ability to perturb the local electron cloud of a molecular structure depends on the relative location of the individual atoms, it follows that the polarizability is a function of the instantaneous position of constituent atoms. For any molecular bond, the individual atoms are confined to specific vibrational modes, in which the vibrational energy levels are quantized in a manner similar to electronic energies. The physical displacement *dQ* of the atoms about their equilibrium position due to the particular vibrational mode may be expressed as:

$$dQ = Q_o \cos(2\pi \nu_m t) \quad \textbf{(4)}$$

where Q_o is the maximum displacement about the equilibrium position. For a diatomic molecule, the polarizability is approximately a linear function of the bond length for small amplitudes of vibration. In terms of the displacements from the equilibrium bond length, that is, in terms of the vibrational coordinate ***Q*** and expanding in a Taylor series one obtains:

$$\alpha = \alpha_0 + (\partial\alpha/\partial Q)_0 Q + \ldots \quad \textbf{(5)}$$

where α_o is the polarizability of the molecular mode at equilibrium position. Based on the vibrational displacement of Eq. (4) , the polarizability may be given as

$$\alpha = \alpha_0 + (\partial\alpha/\partial Q)\, Qo \cos(2\pi \nu_m t) \quad \textbf{(6)}$$

Finally, Eq. (6) may be substituted into Eq. (3), which yields

$$P = \alpha_0 Eo \cos(2\pi \nu_0 t) + (\partial\alpha/\partial Q)\, QoEo \cos(2\pi \nu_0 t) \cos(2\pi \nu_m t) \quad \textbf{(7)}$$

Using a trigonometric identity $\cos\alpha\cos\beta = 1/2\{\cos(\alpha+\beta) + \cos(\alpha-\beta)\}$the above relation may be recast as

$$P = \alpha_0 Eo \cos(2\pi \nu_0 t) + [(\partial\alpha/\partial Q)(Q_o E_o/2)\{\cos[2\pi(\nu_0 + \nu_m)t] + 2\pi(\nu_0 - \nu_m)t]\} \quad \textbf{(8)}$$

The first term in eq. (8) describes a classical dipole oscillating, and hence radiating, at the exciting frequency ν_o. The second and third terms represent "beat" frequencies of the light and molecular vibrational frequencies and describe the Raman scattering at frequencies ($\nu_o - \nu_m$) and ($\nu_o + \nu_m$), respectively. For a polyatomic molecule with several normal modes of vibration, we can extend this simply by summing over the j different vibrational modes

$$P = E_o \alpha_o \cos(2\pi \nu_o t) + \frac{1}{2} E_o \sum_{j=1}^{J} Q_j \left\{\cos\left[2\pi(\nu_o + \nu_j)t\right] + \cos\left[2\pi(\nu_o - \nu_j)t\right]\right\} \quad \textbf{(9)}$$

It is important to note as selection rule of Raman spectroscopy is that $(\partial\alpha/\partial Q)$ must be $\neq 0$,

This condition may be physically interpreted to mean that the vibrational displacement of atoms corresponding to a particular vibrational mode results in a *change* in the polarizability.

One failure of the classical theory is that it predicts that the intensities of the Raman lines at ($\nu_o + \nu_m$) and ($\nu_o - \nu_m$), should be almost the same, while we noted earlier that the line at ($\nu_0 + \nu_m$), has much lower intensity. In the discussion above, α was treated as a scalar that is, as a simple proportionality constant relating the induced dipole moment to the inducing electric field vector. Now the important quantity for a qualitative understanding of infrared absorption intensities, the dipole moment, is a vector involving three numbers $\boldsymbol{\mu} = \mu_x \boldsymbol{i} + \mu_y \boldsymbol{j} + \mu_z \boldsymbol{k}$. In general, it is easy to visualize a vector in three dimensions as an arrow. The polarizability, α, must relate one vector, the electric field, to another vector, the induced dipole moment, where these two vectors are not necessarily parallel. In general, a tensor which involves nine numbers is required for this, eq. (9), and it is a **3** X **3** matrix.

$$\begin{pmatrix} P_x \\ P_y \\ P_z \end{pmatrix} = \begin{pmatrix} \alpha_{xx} & \alpha_{xy} & \alpha_{xz} \\ \alpha_{yx} & \alpha_{yy} & \alpha_{yz} \\ \alpha_{zx} & \alpha_{zy} & \alpha_{zz} \end{pmatrix} \begin{pmatrix} E_x \\ E_y \\ E_z \end{pmatrix} \qquad \textbf{(10)}$$

The physical significance of the tensor can be seen by considering, as examples, the elements in the second row. The diagonal element α_{yy} determines the magnitude of the y component of the induced molecular dipole moment which arises from the y component of the oscillating electrical field. The off-diagonal element α_{yx} determines the contribution to the y component of the dipole caused by the *x* component of the electrical field, while α_{yz} determines the contribution to the y component of the dipole moment arising from the *z* component of the electrical field.If the polarizability tensor is symmetric that implies that $\alpha_{ij} = \alpha_{ji}$ **(i, j, k: = x, y, z)**, there are 6 components of the polarizability tensor, if one of then $\partial\alpha/\partial Q \neq 0$ the vibration is

Raman active. To visualize the equilibrium molecular polarizability α we can draw arrows from common origins which have lengths proportional to the value of α in that particular direction. The heads of all of these arrows will define an ellipsoid. For some purposes it is more convenient to make the length of the arrows proportional to fro or to $\sqrt{\alpha}$ **or** $1/\sqrt{\alpha}$**.**The use α representation is favored. Finally, one can make the polarizability matrix much simpler if this ellipsoid is oriented with its principal axes along the x, y, and *z* axes of the coordinate system used to describe the polarizability.

1.2.4 Previous Work

During the past few years, researchers have dedicated part of their time and efforts to study the detection of explosives, hazardous liquids, and chemical agents on many surfaces and into bottles. Recent work has led to development of methods to couple Raman systems to light collecting systems, i.e., telescopes. In 2003, Sharma et al. developed a version of a visible region, standoff Raman spectroscopic system, using Maksutov-Cassegrain telescope and a pulsed laser (20 Hz, 532 nm, Nd:YAG) [12]. This system was capable of measuring the Raman spectra of benzene in liquid and vapor phase and minerals located at a distance of 4.5-10 m from the telescope.

Sharma et al. in 2005 used a small portable Raman system for standoff detection and identification of various types of organic chemicals including benzene, toluene, ethyl benzene and xylenes (BTEX) [13]. Both fiber optics (FO) coupled and a directly coupled systems of telescope to f/2.2 spectrographs were developed and tested. A frequency-doubled Nd:YAG pulsed laser (20 Hz, 532 nm, 35 mJ/pulse) were used as excitation source. The operational range of the FO coupled Raman system was tested to 66 m, and the directly coupled system was tested

to a distance of 120 m. They also measured remote Raman spectra of two explosives: tri-aminotrinitrobenzene (TATB) and beta-HMX at 10 m standoff distance.

Carter et al. (2005) designed and demonstrate a stand-off Raman system for detecting high explosive materials at distances up to 50 m in ambient light conditions [20]. In the system, light was collected using an 8 in. Schmidt–Cassegrain telescope fiber-coupled to an f/1.8 spectrograph with a gated intensified charge-coupled device (ICCD) detector. A frequency-doubled Nd:YAG (532 nm) pulsed (10 Hz) laser was used as the excitation source for measuring remote spectra of samples containing up to 8% explosive materials. The explosives RDX, TNT, and PETN as well as nitrate- and chlorate-containing materials were used to evaluate the performance of the system with samples placed at distances of 27 and 50 m. Laser power studies were performed to determine the effects of laser heating and photodegradation on the samples.

In 2006 Aunupam et al. obtained Raman spectra of common minerals and organic (benzene, cyclohexane, 2-propanol, naphthalene, etc.) compounds from a small portable instrument at a distance of 10 m in a well illuminated laboratory with a single 532 nm laser pulse of energy of 35 mJ/pulse [19].

In 2009 Patterson et al. identified explosives such as TATP, HMTD, HP, MEKP, NM, NB, and IPN at distances of up to 55m employing a remote Raman system based on a 532 nm pulsed laser source combined with gated detection [21].

In 2012 Angel et al, illustrates the current state of standoff Raman spectroscopy for remote planetary applications, including standoff instrumentation, the technique's ability to identify biologically and geologically important analytes, and the feasibility to make standoff Raman measurements under various planetary conditions. [22].

2. Design and development of remote Raman systems

This chapter focuses on our efforts about the development and design of three kinds of prototypes for remote Raman systems.

2.1 Prototype I.

2.1.1 Raman Instrumentation

A Renishaw Raman spectrometer model RM2000 (Renishaw. Inc, Hoffman Estates, IL,USA), equipped with a Leica microscope (5x,10x, 20 x and 50x objectives), charge-coupled device (CCD) detector and the appropriate optical filters for rejection of satellite plasma lines (laser line filters) and edge filters (RazorEdge™ long wave pass filters, Semrock, Rochester, NY. USA) with vertical transition width of 2.4–2.7 nm were used to block Rayleigh scattered light. This system was employed for the vibrational spectroscopy measurements. Raman spectra of samples were collected in the Raman Shift range of 200-3600 cm^{-1} (0.5 cm^{-1} resolution) employing an integration time from 1 to 30 s (Fig. 3).

Figure 3. Raman Microscope Renishaw RM 2000.

2.1.2 Laser Source

The 514.5 and 488 laser lines of a Coherent, Inc. INNOVA 308 argon ion laser and the 532 nm of a Coherent, Inc. VERDI solid state diode laser system, 6 watts maximum power, solid state diode laser system were employed as excitation sources in continuous mode (CW), both laser are shown in Figure 4.

Figure 4. Continuous wave mode laser system.

2.1.3 Fiber Optic

Premium Grade Xtreme™ solarization resistant (XSR) optical fiber assemblies and reflection/backscattering probes, wavelength range 180-900 nm was used to couple collecting telescope and Raman microscope Renishaw. The diameter of the fiber (Figure 5) was 600 µm AL 1217, Ocean Optics., Inc. (Dunedin, FL).

Figure 5. Fiber optic employed for coupling

2.1.4 Telescope

A Meade ETX-125AT 5.0"/125mm Maksutov-Cassegrain reflective telescope (1900 mm; f/15) with motorized guidance system (Altazimuth Mount, Autostar™ computerized controller), 26 mm (73x) 1.25" eyepiece, 8x25 finderscope was used as light collector. The system was equipped with a tripod and a bench stands to allow for various applications (Figure 6).

Figure 6. Reflective telescope employed to collect the Raman scattered signal.

2.1.5 Remote Raman System Design (Prototype I)

The setup for the prototype I remote Raman system is schematically shown in Figure 7. The ensemble consisted of a Renishaw Raman Microspectrometer, model RM2000 (Renishaw Inc, Hoffman Estates, IL. USA), equipped with a charge-coupled device (CCD) detector and the appropriate optical filters for rejection of satellite plasma lines (laser line filters) and edge filters (RazorEdge™ long wave pass filters, Semrock, Rochester, NY) with vertical transition width of 2.4–2.7 nm were used to block Rayleigh scattered light. The remaining parts were a reflective telescope, a fiber-optic assembly and a continuous-wave single-line/frequency laser system operating at 514.5/488 nm (argon ion, Coherent INNOVA 308) or a 532 nm frequency doubled solid state diode Nd:YAG laser (Coherent VERDI- 6W). The telescope, a MEADE ETX-125,

Maksutov–Cassegrain design, 125 mm clear aperture, 1,900 mm focal length, f/15, was coupled to the Raman spectrometer through the white light microscope using an optical fiber (non-imaging, 600 μm diameter, model AL 1217, Ocean Optics, Inc.). Two lenses were used to collimate the light output from the telescope at the exit plane, from which the objective was removed, and directed it into the fiber-optic bundle. The output of the fiber-optic assembly was directly coupled to the Raman Microscope system via a ×5 objective (Figure 8). Spectra of all targets were measured in the Raman Shift range of 100–3,200 cm^{-1} at laser powers of 25–500 mW and integration times of 1–50 s.

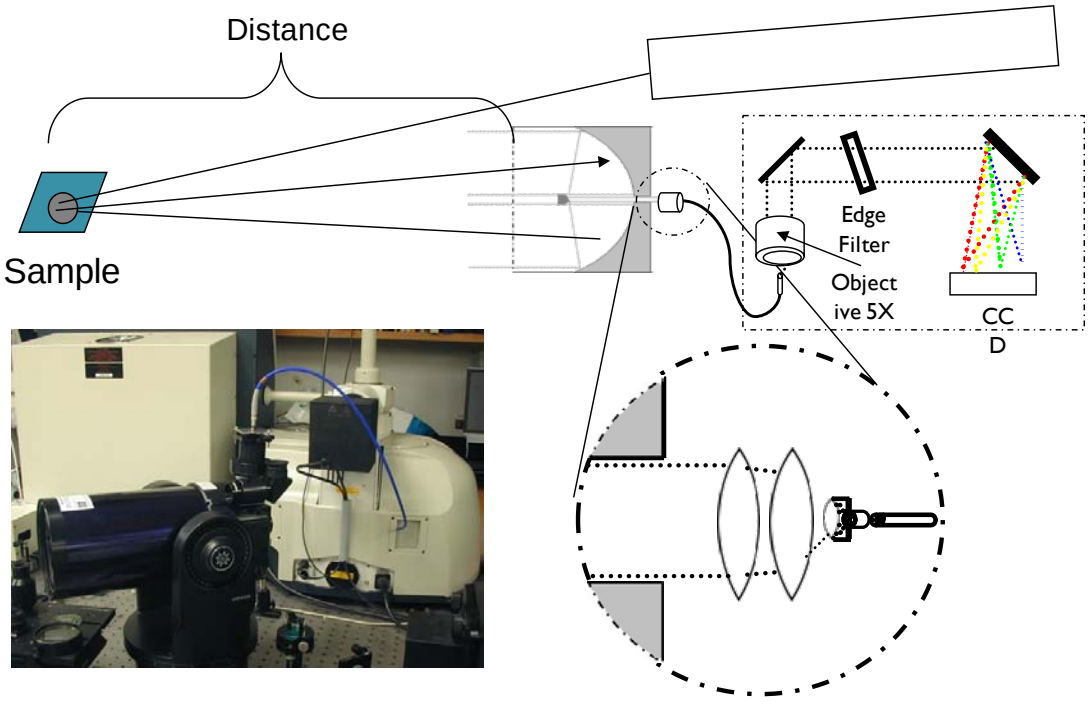

Figure 7. Schematic representation of the Remote Raman System (Prototype I).

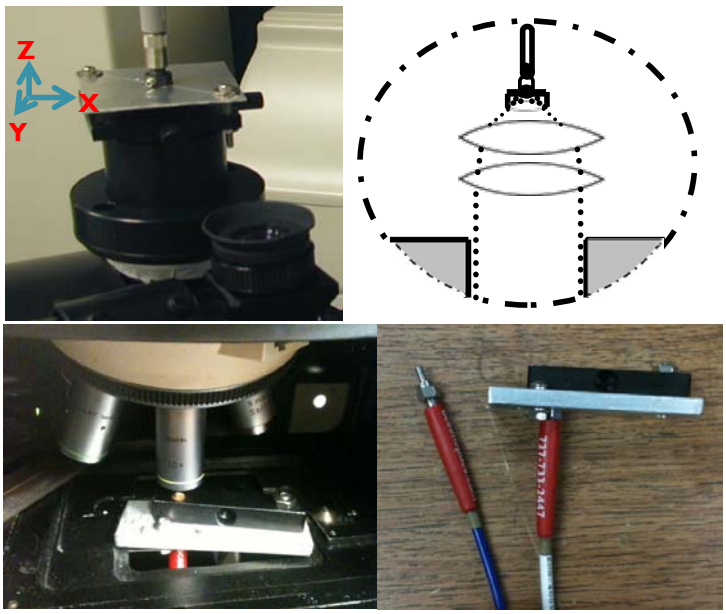

Figure 8. Coupling the collector telescope to the Raman spectrometer through fiber optics assembly.

2.1.6 Remote Raman Spectroscopy measurements

It is important to note that results obtained with the prototype I will not be discussed in detail in this report since they were part of previous works already published. Therefore, only a general description the most relevant results obtained with prototype I will be mentioned below. Prototype I of the RRS was able to detect highly energetic materials (HEM) such as RDX, DNT, TNT, TATP, and C4 in the spectral region of 150 - 3200 cm^{-1} at a distance of 7 m from the telescope using excitation lines from an argon ion laser: 514.5 nm and 488 nm with LOD values of the HEM used as targets. Relatively low amounts ($\leq$ 3 mg) were detected for TNT, DNT, RDX, and C4. For TATP, a relatively large LOD value of 10 mg can be explained in terms of its high surface sublimation rate. In the case of SEMTEX-H, fluorescence from the important formulation prevented to get meaningful spectroscopic information leading to quantification values. (For more detail see [14].

2.2 Prototype II

2.2.1 Raman Instrumentation

The spectroscopic analysis system was assembled using an Andor Technologies spectrograph: Shamrock SR-303i (f/4; focal length: 303 mm; wavelength resolution: 0.1 nm or 4.2 cm^{-1} at the excitation wavelength) equipped with a 1200 grooves/mm Vis region grating. A high performance, back-thinned illuminated CCD camera (Andor Technologies model # DU970N-UVB) with quantum efficiencies of 90% (200 cm^{-1}) to 95% (3200 cm^{-1}) served as Raman scattered light detector.

Figure 9. Andor Shamrock 303i spectrograph system.

2.2.2 Laser Source

The laser system employed to irradiate the sample in the prototype II were the same used by prototype I

2.2.3 Fiber Optic Cable

Optical fiber assembly: 1 way, 100 μm diameter (HOH-UV/VIS), model: *SR-OPT-8014*, (Andor Technologies).

2.2.4 Telescope

The telescope employed to collect the Raman signal was the same used by prototype I.

2.2.5 Remote Raman System Design (Prototype II)

The setup for the prototype II is illustrated in Figure 10. At first sight, the system appears similar to the first prototype, but has significant changes. In particular, the coupling between the telescope and the fiber optic was achieved by the photo port instead of the eyepiece. In this case an Andor spectrograph equipped with CCD was employed as spectrograph and detector

The telescope used in the remote detection system was obtained from the manufacturer as a reflective receiver operating in the VIS region only, According to Figure 11, the telescope was modified to allow for the collection of scattered Raman signals in the near-ultraviolet region, 350-390 nm, by coating the secondary mirror with a thin layer (~ 200 nm) of UV-reflective aluminum. In addition, the minimum focal point where a clear image could be formed was 5 m for prototype I. An anodized aluminum tube with capability for rigidly holding the secondary mirror and moving this mirror to change the focal distance was integrated to the beam path to allow for a reduction of the minimum focal point to 2 m, adding near-field proximity detection capability. The system was successfully tested to 2.2 m target-collector distance.

2.2.6 Standoff Raman spectroscopy measurements

The results obtained with the prototype II will be discussed in the next chapter.

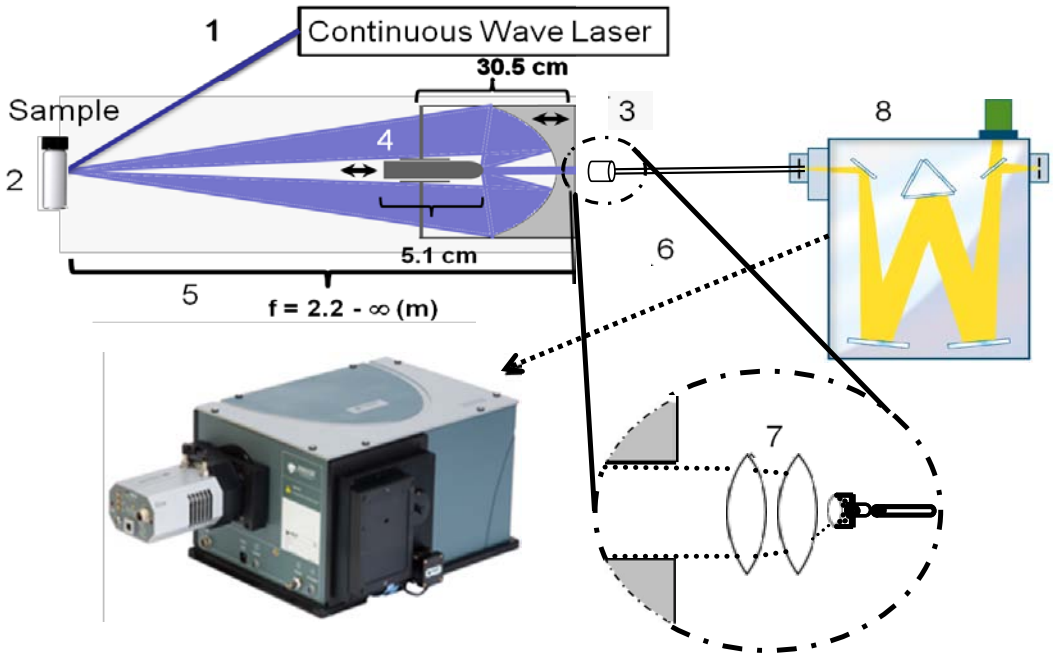

Figure 10. Design details of Remote Raman Detection System (prototype II) : (1) Laser Source; (2) Sample; (3) Reflective Telescope; (4) Variable focus secondary mirror; (5) Remote Distance; (6) Fiber optic coupling; (7) Details of optical coupling; (8) Spectrograph.

Figure 11. Telescope modified.

2.3 Prototype III.

2.3.1 Raman Instrumentation system

The spectroscopic analysis system was achieved by a high efficient Raman Explorer™ spectrograph (Headwall™ Photonics, Inc.) with optical layout for 532 nm excitation line and

aberration-corrected grating designs which eliminate focal plane distortions. High throughput, f/2.4 optics ensure high spectral resolution over multiple input slits across extended wavelength ranges while achieving high signal to noise ratio. Equipped with a gateable, intensified CCD detector (iStar™ ICCD camera, Model DH-720i-25F-03, Andor Technology, Belfast, Northern Ireland) was used as the photon detector. Andor Technology Solis™ software for spectroscopic, imaging and time-resolved studies was used for spectral data acquisition and processing from the intensified and gated CCD detector. Using this software, the data could be acquired in both imaging and spectroscopic modes.

Figure 12. Raman Explorer spectrograph system.

2.3.2 Laser Source

The laser system employed to irradiate the sample in the prototype III was a frequency-doubled 532 nm Nd:YAG pulsed laser system (Quanta Ray INDI Series, Newport-Spectra Physics, Mountain View, CA) was used as the excitation source. The maximum energy/pulse of the laser at 532 nm was 25 mJ, and it operated at a repetition rate of 10 Hz. The pulse width was approximately 5-8 ns, and the beam divergence was less than 0.5 mrad. (Figure 13)

Figure 13. Pulsed laser Nd:YAG

2.3.3 Fiber Optic cable

The fiber optic system was the same employed by prototype II

2.3.4 Telescope

The telescope employed to collect the Raman signal was the same used by prototype I.

2.3.5 Remote Raman System Design (Prototype III)

The setup for the prototype III is looks like the first two prototype, but has significant changes, In this case a Raman explorer spectrograph instead Andor spectrograph, and the excitation source was pulse laser instead continuous wave laser. These changes were very important to get detect compounds at challenging distances such as 141 m.

2.3.6 Optimization of prototype III

2.3.6.1 Effect of the imaging spectrograph

Two imaging spectrograph such as the Shamrock 303i spectrograph (Andor) and Raman Explorer™ (Headwall) were employed in order to improve the maximum collection efficiency of our prototype, these system were selected due to 2 reason, first there are a highly versatile

platform configurable seamlessly with a wide range of light coupling interfaces in-the-field and second for their optical design to allow Image astigmatism correction. In figure 14 illustrates the remote Raman spectra of acetone at 6 m employing a 532 nm excitation wavelength, using 100 to 1000 pulses at spectral region ranging from 300 to 3200 cm^{-1}. Data acquisition was possible leaving constant fiber optic, telescope and ICCD, the only variable was the spectrograph.

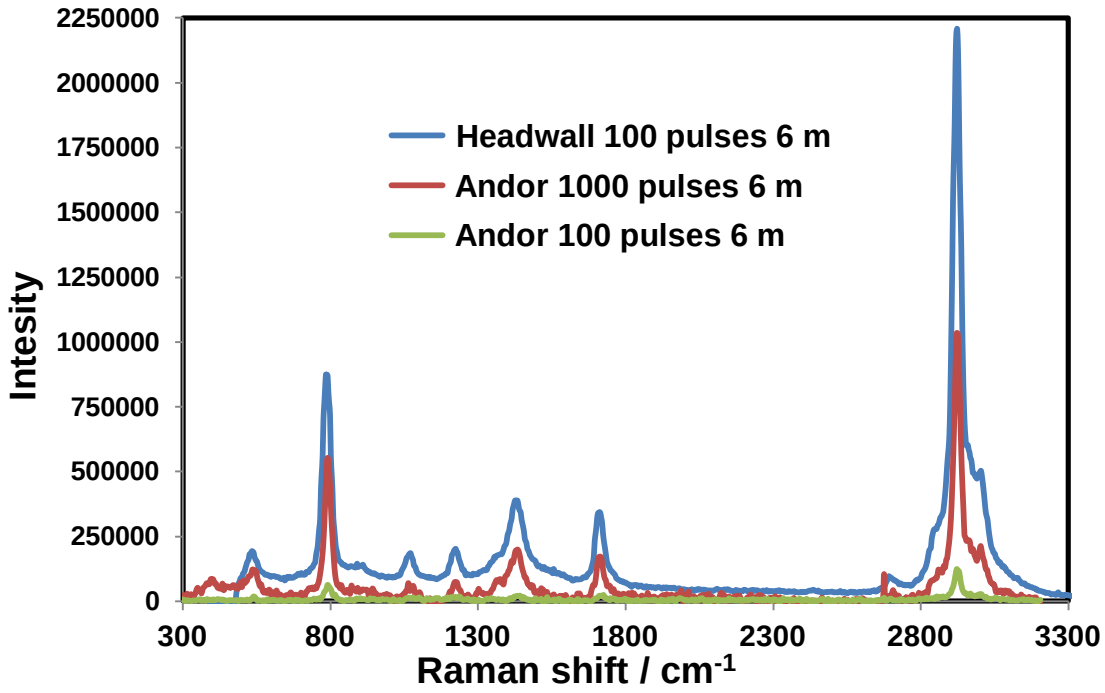

Figure 14. Comparison of the remote Raman detection of acetone employing two different imaging spectrographs.

Comparing the most intensity Raman band spectra of acetone around at 800 and 2900 cm^{-1} corresponding to C-O and C-H stretching symmetric mode respectively. It clearly evident that Raman Explorer spectrograph shows major photonic collection than Andor's Shamrock 303i even when using 1000 pulses for Shamrock 303i not overcome the Raman Explorer intensity obtained with only 100 pulses. The difference between both spectrographs is the *f/#* value. This

parameter is the ratio of focal length to aperture diameter, and determines the light collection ability (and ultimately the throughput) and therefore the magnitude of the Raman signal that reaches the detector plane. This parameter is 2.8 and 4.0 for the Raman Explorer and Shamrock 303i, respectively, which means that at lowering *f*/# value near a 1 significantly increases light collection. Lower f/# requires shorter focal length or larger optics. Another advantage of the Raman Explorer spectrograph consists in the use of a novel aberration-corrected concave grating which produces minimal image blur over the full CCD focal plane with exceptionally high signal to noise efficiency. It is very important to note that the limiting factor of the Raman Explorer spectrograph is that it only works with a 532 nm laser as excitation line, situation does not occur with Shamrock 303i which has a triple grating turret which can be able to make measurements in the UV-VIS-NIR regions.

2.3.6.2 Range dependence of TNT detection

Diffraction phenomena of the light while traveling long distances in free space makes the laser beam lose some degree of collimation allowing the beam spot to increase with distance. To determine this effect on our system we evaluated this result in the remote detection of TNT. Figure 15 illustrates a pattern where the circle represents the sample size diameter (25 mm) and the elliptical area shaded in green represents the outline of the beam spot where the dashed line represents the loss of collimation as distance increases. It is important to note that to collect efficiently the Raman scattered light from the sample it is necessary that the laser spot area should be less or equal than to the area. Figure 16 shows Remote detection of TNT at different distances ranging from 8 to 60 m, employing a 532 nm excitation wavelength, using 100 pulses at spectral region ranging from 500 to 3200 cm^{-1}.

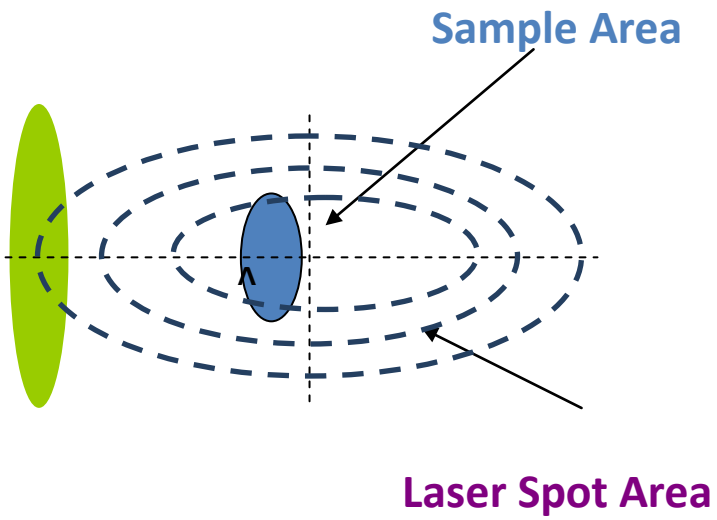

Figure 15. Diffraction effects in remote sensing by comparing sample areas and laser spot

It is evident that in the range from 8 to 30 m distances the spectral information of TNT and its respective vibrational modes have good signal to noise ratios (S/N). Above 30 m one observes a significant reduction of the signal to noise is observed. This is due to loss of collimation problems mentioned above which implies that the area irradiated by the laser increases significantly, meaning that the laser spot area was much larger than the sample area, resulting in lower power/area. According to these results the remote detection of a sample of TNT of 25 mm diameter 30 m away from the excitation source loses scattering strength and therefore suggests the implementation of an optical system that allows the correction of this phenomenon: a beam condenser.

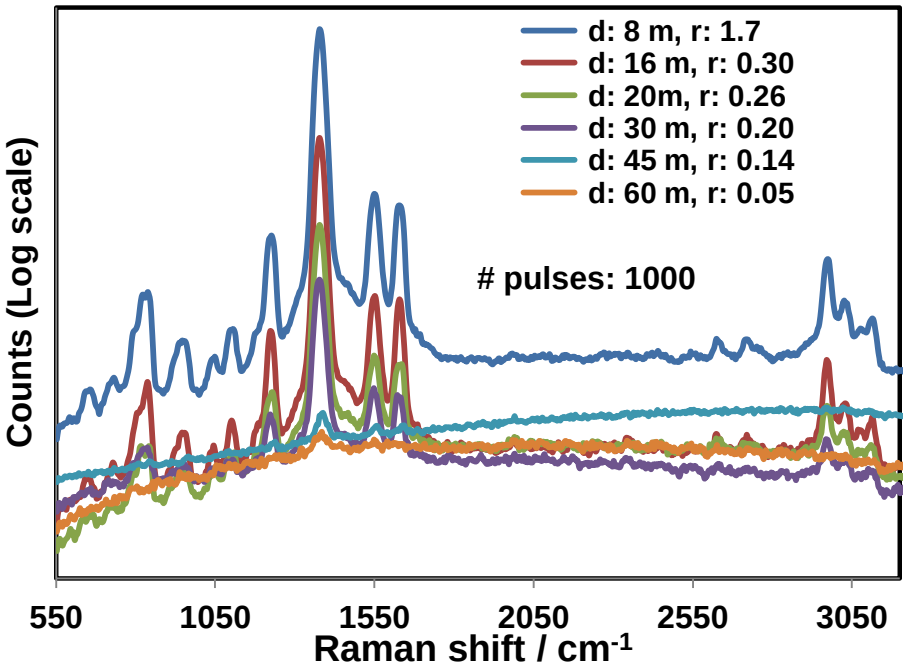

Figure 16. Remote detection of TNT at different distances using several sample/laser area ratios

2.3.6.3 Sample size effect

Another experiment was carried out, in order to observe the effect of sample size. Figure 17 shows a TNT sample container of 25 mm in diameter. On its right, a mechanical iris was used to reduce the diameter of the sample from 25 to 2 mm. Figure 18 illustrates the remote detection of TNT at 16 m while varying the size of the sample, using 100 pulses of a 532 nm laser as excitation source. The spectral region shown goes from 500 to 3200 cm^{-1}. This representation shows the detection (logarithmic scale intensity) of this energetic material and it is evident observe the most relevant vibrational modes of TNT at diameters from 25 to 4 mm, a significant decrease of the Raman signal with absence of vibrational modes and increase background band around 2340 cm^{-1} was observed in sample size with diameter below 4 mm (attributed to Hg from fluorescent lamps).

Figure 17. Sample size effect in the remote detection of TNT at 16 m

The results show that the sample size plays a significant role in remote sensing and even sample size with diameter of 2 mm was achieved according to the Raman band mode at 1350 cm^{-1} for C-NO_2 symmetric stretch of the explosive.

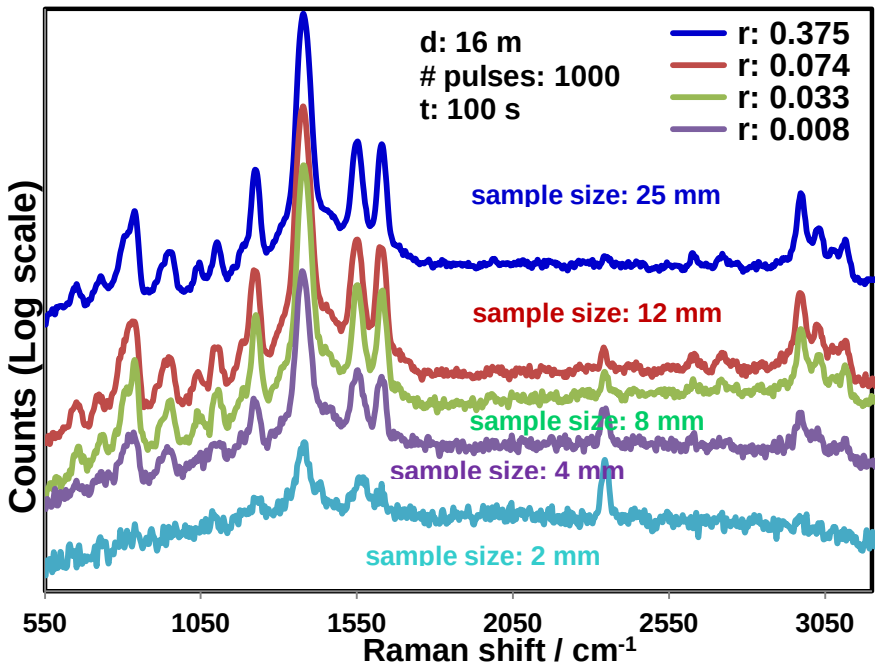

Figure 18 Remote Raman detection of TNT at different sample sizes.

3. REMOTE DETECTION OF HAZARDOUS LIQUIDS CONCEALED IN GLASS AND PLASTIC CONTAINERS

This chapter focuses on detections of hazardous liquids such as liquid explosives, flammables, toxic industrial compounds (TIC) and chemical warfare agents (CWA) in commercials bottles. These compounds can be used as tools against troops and/or civilians by terrorist organizations or individuals. Many of these chemicals are highly exothermic, corrosive or can cause irreversible damage to organs by inhalation or contact even at low concentrations. These liquids are easily concealed within common household products and brought into a public area such as buildings, transportation terminals or an aircraft. Some of these chemicals are capable of doing considerable damage to property or human health even in low quantities.

3.1.1 Material

The commercial liquid products employed in this study were: Kiwi-Strawberry flavored Snapple® (distributed by the Snapple Group USA and Pacific Snapple Distributors, NY), Dasani® water (distributed by Coca Cola Puerto Rico Bottlers), Heineken® (imported by Mendez & Company, PR) and Malta India® (malt beverage manufactured by India Brewery, Mayaguez, PR), the respective bottles are shown in Figure 14. The hazardous materials considered in this work were: acetone, methanol, dichloromethane and 20% hydrogen peroxide in water (Fisher Scientific International, Chicago, IL). Dimethylmethyl phosphonate (DMMP) was obtained from Sigma-Aldrich Chemical Company, St. Louis, MO. DMMP is a structural analog of the nerve agent Sarin and it is commonly used as a Chemical Warfare Agent Simulant

(CWAS) for vibrational spectroscopy and other physical properties measurements.

Figure 19. Common plastic and glass bottles were used as suspicious items were the original liquid was replaced by a hazardous chemical

The original liquids in the bottles were replaced by 30 mL of the potentially hazardous chemicals used. Then the bottles were placed at the remote location at 20 ft. from the collector telescope. The spectra were recorded in the Raman Shift range of 100-3200 cm^{-1}. In most cases, only the fingerprint region of 200 to 2000 cm is shown. This is the region in which the vibrational signatures for the hazardous chemicals are located. Table 1 summarizes properties of the containers used for the study.

Table 1. Common Containers Evaluated with Remote Raman System

Product	Material	Color	Thickness (mm)
Water	Plastic (PET)	Clear	0.22 ± 0.02
Fruit juice	Glass	Clear	1.92 ± 0.42
Malt beverage	Glass	Amber	2.28 ± 0.44
Beer	Glass	Green	2.02 ± 0.47

3.2 Instrumentation

Remote Raman experiments were performed using Prototype II remote Raman detection system with the strong blue line at 488 nm of an argon ion laser INNOVA 310-8 (Coherent, Inc.). The laser beam was focused on the sample at a distance of 20 ft. from the target to the collection optics. The scattered radiation was collected using MEADE ETX-125, (Maksutov-Cassegrain; D: 127 mm; F: 1900 mm) telescope that was optically coupled to the light spectrometer entrance slit with an optical fiber (non-imaging, 600 μ diameter, model AL 1217, Ocean Optics, Inc.). An Andor Technologies spectrometer/spectrograph: Shamrock SR-303i (aperture: f/4; focal length: 303 mm; wavelength resolution: 0.1 nm or 4.2 cm^{-1} at the excitation wavelength) equipped with a1200 grooves/mm grating. A high performance back illuminated CCD camera (Andor Technologies model # DU970N-UVB) with quantum efficiencies of 90% (200 cm^{-1}) to 95% (3200 cm^{-1}) served as scattered Raman light detector. Two lenses were used to collimate the light output from the telescope at the exit plane and directed it into the fiber optic bundle. A Semrock laser notch filter placed at the entrance slit of the monochromator was used to reject the Rayleigh scattered radiation. Spectra of all compounds were collected with the laboratory lights off to avoid interference of lab fluorescent lamps illumination. These conditions are typical for experiments with continuous wavelengths (CW) lasers.

3.3 Results and discussion

3.3.1 Remote detection of methanol, dichloromethane and DMMP in water clear plastic bottle

Drinking water is commonly sold in a variety of clear plastic bottles and it would be relatively simple to substitute the contents of these bottles with clear translucent hazardous

chemicals and use the device as a weapon of mass destruction (WMD). Thus, the first experiments consisted of differentiating the original contents of the commercial liquids used from other clear liquids placed in lieu of the original bottle contents. The water contents of clear plastic bottles were replaced with mixtures of water and methanol and measured by RRS at 20 ft. typical results of this experiment is shown in Figure 15. As expected, water has very low Raman activity and there are no noticeable prominent peaks that could interfere with target analytes vibrational signatures. The peaks at 1015 cm^{-1} and 1460 cm^{-1} confirm the presence of methanol in the mixture.

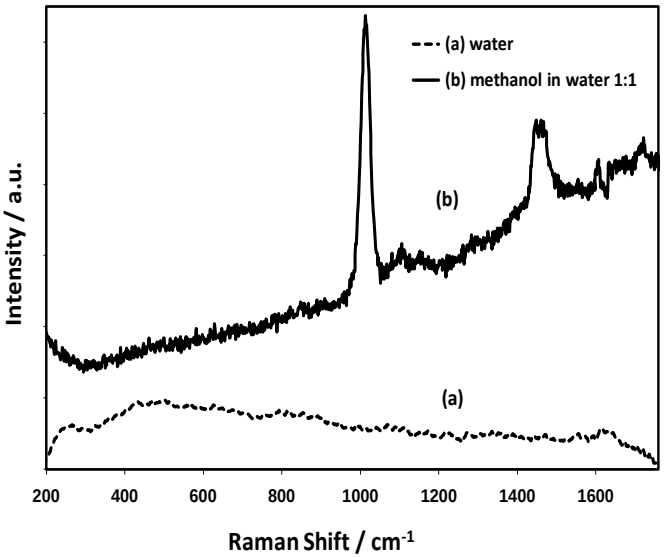

Figure 20. Raman spectra of liquids contained in clear plastic bottle: (a) water; (b) methanol in water, 1:1 mixture. Spectra were acquired at 20 ft. target-collector distance using 630 mW laser power, 1 accumulation, and 10 s integration time.

Next the content of the bottles were replaced with a series of clear liquids. The spectroscopic signatures of the chemicals were easily obtained at 1 acquisition of 10 s integration time. Results obtained for some of the liquids studied are illustrated in Figure 16. All spectra were measured at a constant remote distance of 20 ft.

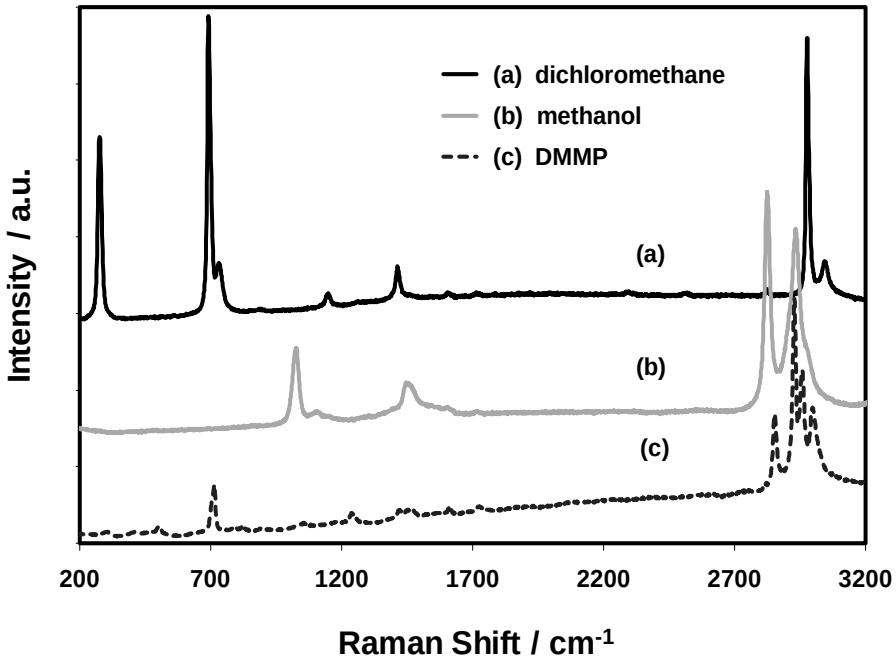

Figure 21. Remote Raman spectra of hazardous liquids contained in clear plastic bottles: (a) dichloromethane; (b) methanol and (c) DMMP. Spectra were acquired at 1 accumulation, 10 s integration time using a laser power of 630 mW measured at head.

3.3.2 Remote Raman detection of DMMP in Snapple Kiwi-Strawberry juice

The second set of experiments consisted in studies of colored liquids in clear glass bottles. Snapple™ Kiwi-Strawberry juice was mixed with DMMP for this study. As shown in Figure 22, the mixture and the original beverage both exhibited a moderate level of fluorescence interference that shows as a steep baseline, probably caused from the highly colored components of the beverage. However, this fact did not prevent the spectroscopic measurements and it was possible to identify DMMP in a 1:1 mixture with the beverage. The peak at 715 cm^{-1} is characteristic of a stretching mode involving phosphorus-oxygen atoms in DMMP. When a hazardous liquid was used to replace the fruit juice in a Snapple™ bottle (clear glass), the

difference in spectroscopic signatures measured could be used for identification of the threat compound, even in the presence of a moderately strong fluorescent background.

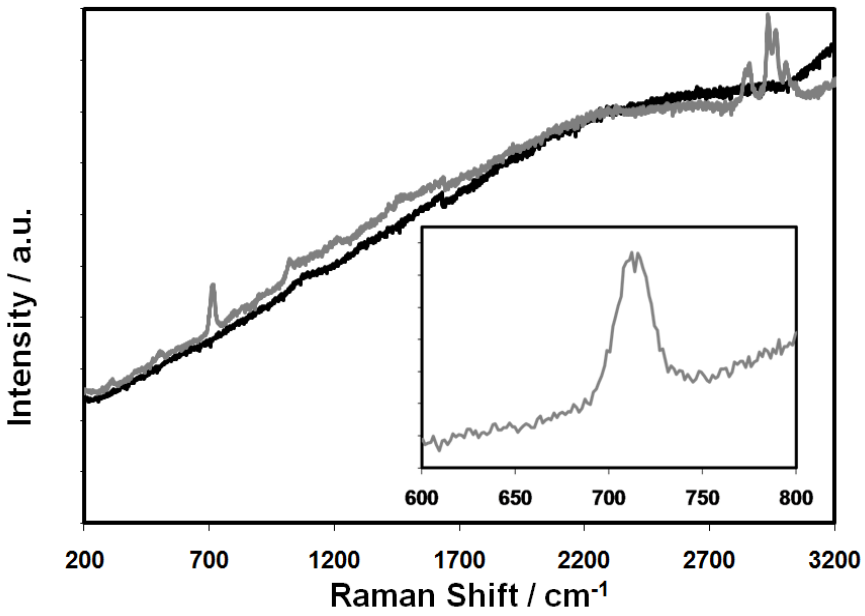

Figure 22. Remote Raman spectra of liquids contained in a clear glass bottle: (a) Snapple Kiwi-Strawberry juice (b) mixture of juice and DMMP, (c) area of characteristic peak of DMMP at 715 cm-1, Conditions: laser power (head) 630 mW; 1 acquisition. Conditions: laser power (head) 630 mW; 1 acquisition; 30 s integration time.

3.3.3 Remote Raman Detection of TATP precursors

In Figure 23 acetone, hydrogen peroxide and a mixture of hydrogen peroxide and acetone were detected though the walls of clear glass of the Snapple™ bottle. The most prominent band for hydrogen peroxide is the band at 880 cm^{-1}.

This strong band is a marker for peroxidic compounds since it corresponds to the O-O stretching mode. Acetone can be easily identified by the C=O stretching at 1700 cm^{-1}. The

incipient formation of the reaction products between the two liquids can be easily observed by shifts in the vibrational bands and formation of new signals that can be attributed to the presence acetone peroxide (AP) cyclic acetone based aliphatic peroxides. The hydrogen peroxide/acetone mixture is the essential part of the components needed to prepare triacetone triperoxide (TATP), a very sensitive and powerful explosive used by terrorists as homemade explosive (HME) as in the case of the shoe bomber in 2001 and the London bombing in 2005.

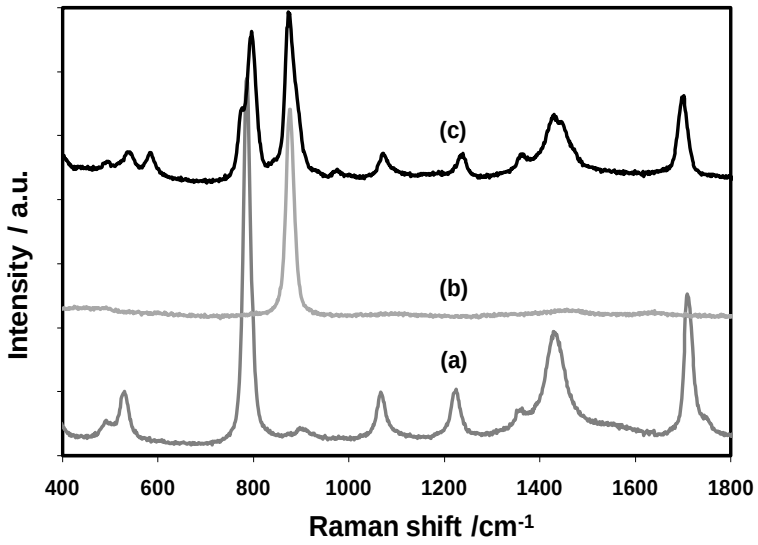

Figure 23. Raman spectra in clear glass bottle of: (a) acetone (b) hydrogen peroxide, (c) mixture of acetone and hydrogen peroxide. Laser power 630 mW, 1 acquisition, 10 s.

The most important bands in the Raman spectrum of TATP appear in the Raman Shift range of 860-1000 cm^{-1} corresponding to peroxide O-O stretching modes. The low-frequency bands near 550-600 cm^{-1} corresponds to the O-C-O bending motion. Together these bands are markers of cyclic peroxidic compounds like TATP [19]. For the prepared mixture, the Raman spectra show bands at 1700 cm^{-1} and 760 cm^{-1} from unreacted acetone. The same set of hazardous chemicals was transferred to an amber glass malt beverage bottle for the Remote Raman measurements. Figure 24 shows the Raman spectra of acetone, methanol and mixtures of

hydrogen peroxide/acetone and water/DMMP. The increase in baseline noise reflected by the decrease in signal to noise ratio (S/N) is a consequence of the low light transmission through the walls of the amber glass bottle. This is probably due to the constituents of the glass used for making the bottle. Vibrational signatures were obtained, however the areas under the vibrational peaks were lower than those of the same mixtures in other containers. These S/N values were increased using higher laser powers and longer acquisition times.

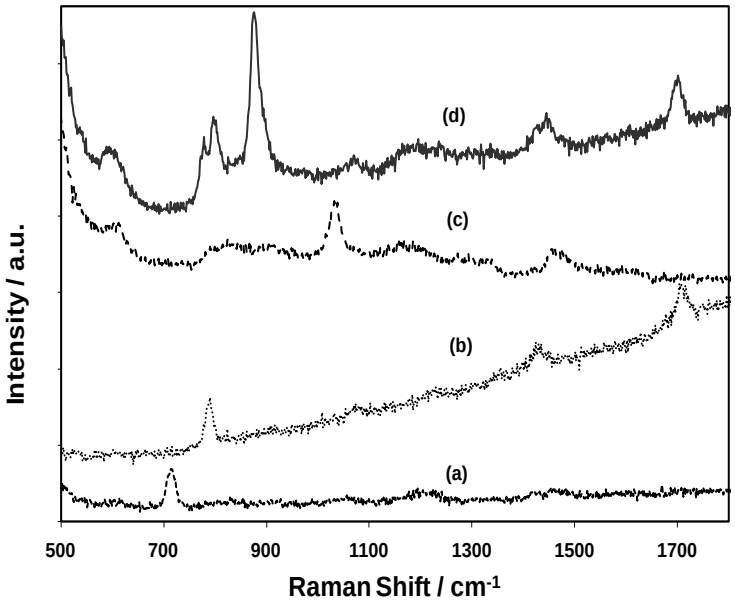

Figure 24. Raman spectra in amber glass bottle of: (a) mixture of water and DMMP; (b) acetone; (c) methanol; (d) mixture of acetone and hydrogen peroxide. Laser power 500 mW, 2 acquisitions, 20 s

3.3.4 Effect of color and thickness of the bottle

Remote Raman spectra of DMMP, a CWA simulant, were measured inside glass bottles. Typical spectra obtained are presented in Figure 25. The spectra of DMMP with the same acquisition parameters are compared for clear, green and amber glass bottles. The reduced signal obtained with colored bottles is clearly illustrated. Since the 714 cm^{-1} vibrational signature of DMMP is characteristic of the CWA simulant it was used to study the effect of the integration

time at fixed laser power of 500 mW (measured at head) for single acquisition runs. The composition of the glass used in the three types of glass bottles used has a marked effect on the detection of the threat chemical.

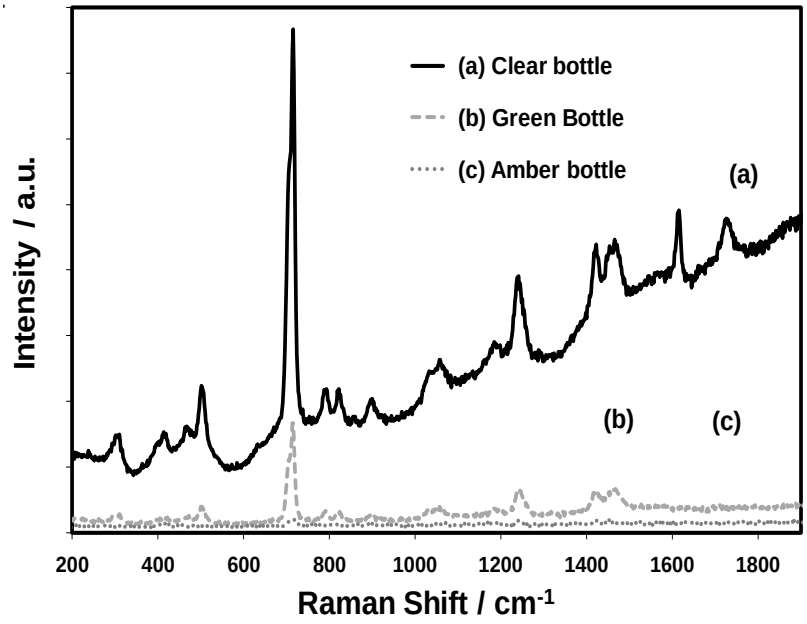

Figure 25. Remote Raman spectrum of Chemical Agent Simulant DMMP measured in different glass bottles at a distance of 20 ft from the collection optics. (a) clear plastic bottle; (b) amber glass bottle; (c) green glass bottle. Laser source: Ar+ 488 nm, power 500mW (head), 10 s, 1acquisition.

A significant reduction of the backscattered Raman is observed for green bottles and this even lower for amber colored bottles. However it was possible to demonstrate that hazardous chemical could be detected and identified by their vibrational signatures regardless of the bottle material.

The signal reduction due to the container wall material was studied by measuring the transmittance properties of the bottles. Figure 26 presents the percent transmittance of light radiation by the container wall material. The signal reduction depends on type of material

(additives used to color the glass) rather than thickness. A vertical line at 488 nm represents the excitation wavelength used to measure the Raman spectra of the target analytes used. Clear, green and amber glass bottles have comparable thicknesses (as shown in Table I), however there is 80% more absorption by the walls of amber glass bottles.

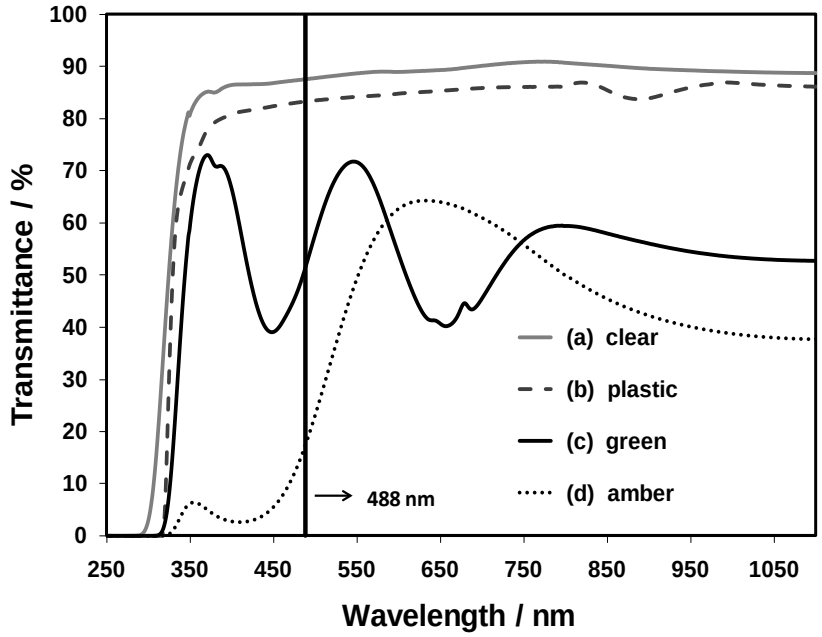

Figure 26. Effect of bottle material: percent of radiation power transmitted by the walls of the container. The laser wavelength used in the experiments is shown as a solid vertical line. The vertical dashed line represents the maximum wavelength range of scattered radiation

As shown in Table 2, a single acquisition of 1s integration through clear glass or plastic bottles is as significant as an acquisition of 5s for green glass and 15s for amber glass. These and other parameters related to the composition of the bottles walls and the target analytes have to be considered in the design of a semi-automatic, “turn-key” system for remote detection of concealed hazardous liquids.

Table 2. DMMP 714 cm^{-1} average peak areas for single acquisition runs.

Wall material	1 s	5 s	15 s
Clear glass	5,000	21,200	64,300
Clear plastic	3,500	16,500	50,700
Green glass	900	3,600	12,300
Amber glass	400	1,500	5,100

3.4 Summary

Vibrational spectroscopy signatures of chemicals can be used to discriminate between suspicious liquids disguised as the original bottle content. To determine the possibility of this event, a Remote Raman Spectroscopy detection system was used to monitor if the content of a commercial product is the intended one or if instead it contained a hazardous material that could be used as a threat. The samples were examined in plastic and glass bottles at a remote target to collector distance of 20 ft. Although the results obtained depended to a certain extent on the composition of glass examined, pure threat chemicals could easily be detected in all bottles tested. The data for a mixture of a CWA and a fruit juice suggest that detection of 10%-20 % of the CWA can be attained under such conditions. This study does not pretend to establish the limits of detection of the technique but it rather presents the potential of a Raman based remote detection system for suspicious consumer products screening. The transmission of the probe laser beam through the walls of the bottles followed the order: clear glass > plastic > green glass > amber glass. The technique under development could serve as a tool for alerting security personnel about the transport or malicious concealment of threat chemicals that could be used as threats to people or property. Current efforts include the application of mathematical algorithms and discriminant functions to reduce fluorescence and other interferences from highly colored

liquids and obtain lower detection limits. Using this technique, the inspection of the contents of bottles can be done remotely, thus reducing the risks of personal and property damage.

4. REMOTE CONTINUOUS WAVE AND PULSED LASER RAMAN DETECTION OF CHEMICAL WARFARE AGENT SIMULANTS AND TOXIC INDUSTRIAL COMPOUNDS

This chapter, we reported our efforts on the design, assembly and testing of two remote Raman Systems: one operating with continuous wave (CW) laser lines and the other using a pulsed laser system. The collector telescope was modified to operate with both visible (400 - 700 nm) and near-ultraviolet ((NUV) 200 - 400 nm)) excitation, improving the detection of hazardous compound from initial measurements of 6-8 m to distance of 141 m away.

4.1.1 Experimental

4.1.2 CW Remote Raman Spectroscopy System set-up

The visible CW laser excitation system has been described in Prototype II. Remote Raman measurements of TIC, which are typically strong inelastic scatterers, were initially carried out using this system without any modifications at a fixed target-collector distance of 6.6 m with visible light excitation. In order to measure remote Raman spectra in the NUV and to measure at closer target-collector distances, several modifications had to be made to the receiver reflector telescope. The modified experimental setup for the prototype RRS-based system is shown schematically in Figure 9. The spectroscopic analysis system consisted of an Andor Technologies Shamrock SR-303i spectrograph, which was equipped with a high quantum response charge-coupled device detector (CCD, Andor Technologies model Newton™ DU-970N- UVB), the appropriate filters for the rejection of satellite plasma lines (laser line filters), and a laser radiation filter designed to block Rayleigh scattered light (edge filters, obtained from Semrock, Inc.

Rochester, NY). The nominal detector efficiencies were 95% (532-570 nm), 93% (514.5 nm), 90% (488 nm) and 35% (350-390 nm).

The other necessary components were a reflective telescope used as a collector or signal receiver, a fiber optic assembly, and a single-line laser system operating at 351.1, 363.8, 488.0, 514.5 and 532 nm (Coherent INNOVA 308, Coherent SABRE 25/7 argon ion laser systems; Coherent VERDI-5 solid state diode laser system). The telescope used was a MEADE ETX-125 Maksutov-Cassegrain design (125 mm clear aperture, 1900 mm focal length, *f*/15). The reflecting collector was coupled to the Raman spectrometer with a non-imaging, 600 μm diameter optical fiber (model AL 1217, Ocean Optics, Inc., Dunedin, FL). Two lenses were used to collimate the light from the telescope output, from which the focusing objective was removed, and direct it into the fiber optic assembly. The output of the fiber optic assembly was directly coupled to the Raman spectrometer entrance slit.

The telescope used in the remote detection system was obtained from the manufacturer as a reflective receiver operating in the VIS region only. It was modified to allow for the collection of scattered Raman signals in the near-ultraviolet region, 350-390 nm, by coating the secondary mirror with a thin layer (~ 200 nm) of UV-reflective aluminum. In addition, the minimum focal point where a clear image could be formed was 5 m. An anodized aluminum tube with capabilities of rigidly holding two quartz lenses and moving the lenses to change the focal distance was integrated to the beam path to allow for a reduction of the minimum focal point to 2.0 m adding near-field proximity detection capability. The system was successfully tested at a 2.2 m target-collector distance. Although RRS spectra are not shown, data is but included as part of system performance tests. The changes made to the collector telescope are also illustrated in Figure 10.

4.1.3 Pulsed laser Remote Raman System set-up

The pulsed laser standoff Raman system used the components of the CW system with the exception of the excitation source and the spectrometer detector. A frequency-doubled 532 nm Nd:YAG pulsed laser system (Quanta Ray INDI Series, Newport-Spectra Physics, Mountain View, CA) was used as the excitation source. The maximum energy/pulse of the laser at 532 nm was 200 mJ, and it operated at a repetition rate of 10 Hz. The pulse width was approximately 5-8 ns, and the beam divergence was less than 0.5 mrad. A gateable, intensified CCD detector (iStar™ ICCD camera, Model DH-720i-25F-03, Andor Technology, Belfast, Northern Ireland) was used as the photon detector. Andor Technology Solis™ software for spectroscopic, imaging and time-resolved studies was used for spectral data acquisition and processing from the intensified and gated CCD detector. Using this software, the data could be acquired in both imaging and spectroscopic modes.

4.1.4 Samples and Remote Raman Experiments

The remote system was tested using TIC and CWAS. The toxic industrial compounds investigated were chlorobenzene, toluene benzene, carbon disulfide, carbon tetrachloride and cyclohexane (all from Fisher Scientific International, Chicago, IL). The chemical warfare agents simulants (CWAS) studied were dimethylmethyl phosphonate (DMMP, 99%, Fisher Scientific International, Chicago, IL), 2-chloroethyl ethyl sulfide (2-CEES, Sigma Aldrich Chemical Company, St. Louis, MO), and 2-(butylamino)-ethanethiol (2-BAET, Sigma-Aldrich). For CW remote detection experiments, pure liquid samples were transferred to 5 mL glass or quartz vials and placed 6.6 m away from the receiver telescope/excitation laser. The spectra of all compounds were collected with the laboratory lights off to avoid background light and mercury lines from

fluorescent lamps. The spectra were acquired in the Raman Shift range of 100-1800 cm^{-1} at laser powers (measured at head) ranging from 0.05 to 1 W and a single acquisition with integration time of 1-30 s. Quantification studies of DMMP/water solutions were carried out at a fixed 6.6 m target-collector distance using the CW RRS system only.

Standoff detection experiments on DMMP at 35 m and cyclohexane at 60, 90 and 141 m were carried out using pulsed mode laser RRS system. DMMP was contained in clear glass bottles 2.5 cm in diameter and 5.0 cm high. For acquisition of remote Raman spectra of cyclohexane at the longest distances, the sample was contained in clear glass bottles that were 7.5 cm in diameter and 15.2 cm high. The criterion used for changing vials at longer distances was that the beam diameter at the sample would be smaller than the cross section of the vials containing the samples. Liquids were remotely detected in the spectroscopic range of 500 to 3200 cm^{-1} using 1 to 1000 pulses of 532 nm excitation wavelength, with pulse energy of ~ 200 mJ.

4.2 Results and Discussion

4.2.1 Remote CW Raman Spectra of TICs

Important industrial solvents and starting materials used for manufacturing in the petrochemical, pharmaceutical, electronic, and other chemical industries are highly flammable, lachrymatory, toxic, mutagenic or carcinogenic. Some of these compounds are used in amounts that constitute potential threats. Thus, it is vital to find ways of monitoring these compounds in air and in their container bottles. Remote Raman systems offer new and simple alternatives to carry out these monitoring processes by remote sensing of the liquid and even the vapor phase (UV Raman). Figures 22 and 23 illustrate the remote CW Raman spectra of organic solvents,

some of which are constituents of hydrocarbons found in petroleum-processing plants. All of the spectra were collected at a distance of 6.6 m from the telescope under laboratory conditions using low illumination. Samples were detected using 514.5 nm laser line excitation at 1W (measured at head) using a single acquisition and integration time of 10 s.

The most prominent feature common among all the spectra in Figure 27 is the aromatic ring-breathing mode at ca. 1000 cm^{-1}. This strong Raman band is characteristic of the symmetric stretch mode of the benzene ring at 992 cm^{-1} [23- 26]. In the case of toluene and chlorobenzene, the same band appeared at 1003 cm^{-1}. Another characteristic band of toluene was found at 786 cm^{-1}. The C-Cl stretching mode of chlorobenzene was clearly observed at about 700 cm^{-1} in the Raman Shift spectrum of this TIC.

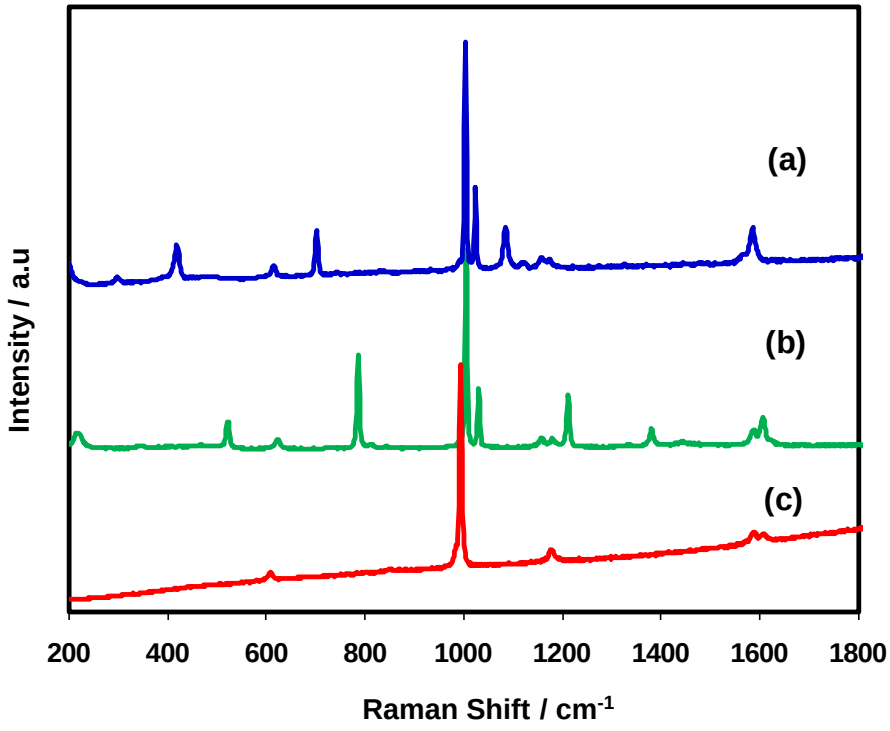

Figure 27. Remote Raman spectra of aromatic TICs in the spectral region of 150-1800 cm^{-1} (a) chlorobenzene (b) Toluene ; (c) benzene. Conditions: target-collector distance: 6.6 m; CW laser source: 514.5 nm 1 W; one acquisition time of 10 s integration.

Several organic solvents widely used in industry, teaching, and research labs were also studied. Among these solvents were carbon disulfide, carbon tetrachloride and cyclohexane. Typical Remote Raman spectra are shown in Figure 28. All of these compounds have characteristic physical and chemical properties. Cyclohexane is typically used as a calibration standard for the Raman Shift axis in dispersive instruments, particularly in Raman studies of liquids [27]. In this work, the Remote Raman spectra of these compounds were measured for liquids contained in 5 mL clear glass vials in the 150–1800 cm^{-1} range at a standoff distance of 6.6 m (Fig. 23).

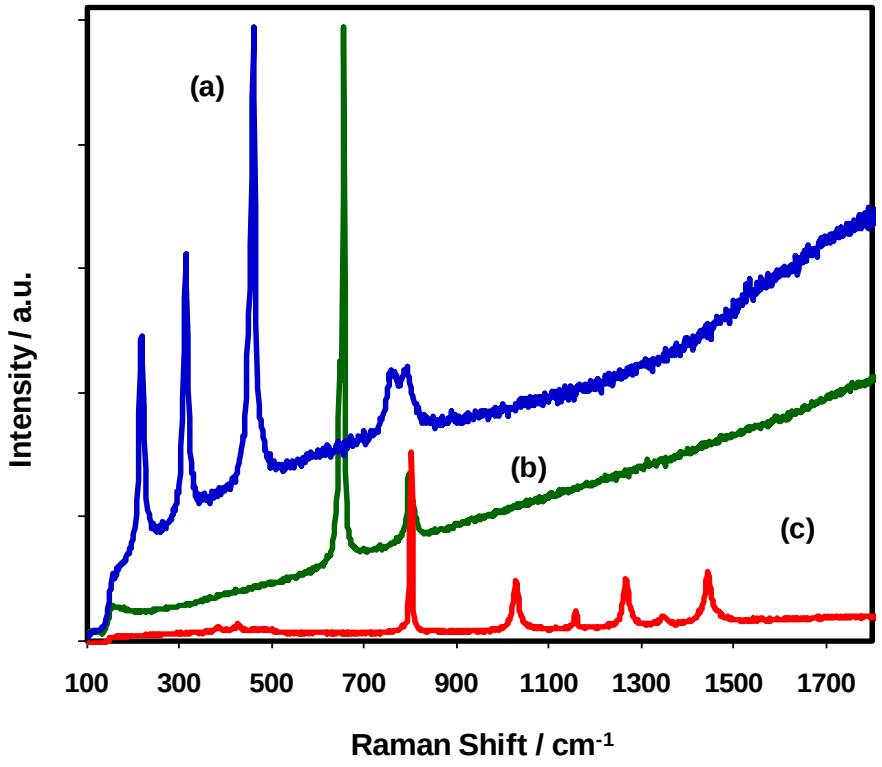

Figure 28. Remote Raman spectra of aliphatic TICs: (a) carbon tetrachloride; (b) carbon disulfide; (c) cyclohexane. Conditions: spectral range 150-1800 cm^{-1}; target-collector distance 6.6 m; CW laser 514.5 nm 1 W; one acquisition time of 10 s integration.

In Figure 28, it is possible to identify carbon disulfide by its very strong (highly symmetric nature) peak at ca. 655 cm^{-1}, corresponding to the C-S symmetric stretching mode [28]. Carbon tetrachloride shows its three main Raman active peaks. The most important band for CCl_4 appears at 461 cm^{-1}. This band is attributed to C-Cl symmetric stretching mode [29]. According to the literature, cyclohexane is characterized by four prominent bands in the 800-1650 cm^{-1} region: a very strong peak at 801 cm^{-1} due to the C–C skeletal breathing mode, the weak peak localized at 1029 corresponds to C–C stretching modes, and other, weak peaks that appear at 1260 and 1445 cm^{-1} due to twisting and scissoring modes [27, 30].

4.2.2 Performance of modified CW Remote Raman system

The Continuous Wave (CW) Standoff Raman System was originally designed to measure Raman Shift spectra excited at visible light frequencies (514.5 and 488.0 nm) at a fixed remote distance of 6.6 m. This was based on two main factors: maximum standoff distance due to restrictions based on laboratory space and minimum focal distance of the visible wavelength reflective telescope used as receiver. After successful measurements under the original operating conditions of HE, HME [28] and TICs (the present study), the system was switched operate in the near-ultraviolet region (NUV), and the signal receiver (telescope) was modified to operate as a close field (proximity) detector (1-2 m). After making the necessary changes, the remote detection system was subjected to the challenging task of detecting extremely low cross-section liquids: CWASs.

Figure 29 shows results of the remote detection system for the intensities of the Raman bands of benzene (ring breathing mode at 992 cm^{-1}) and DMMP (C-P stretch at 715 cm^{-1}) at various distances from 2 to 7 m using a CW argon ion laser excitation line at 363.8 nm. The

dependence of the band intensities for the most prominent signals of benzene (used as primary external standard) and DMMP were plotted and then a line was fitted to the data as a function of the target-receiver distance using Statgraphics-Centurion™ data analysis and statistical software package (StatPoint, Inc., Herndon, VA). The resulting fits, shown in Figure 24, were non-linear, as expected, and compared favorably with the data. The decrease of the Raman intensity of the benzene and DMMP peaks with increasing distance is partially attributed to the $1/R^2$ dependence of the remote Raman signal with standoff distance. However, the signal losses are also related to near-field effects and to partial defocusing of the image on the slit of the spectrograph [32].

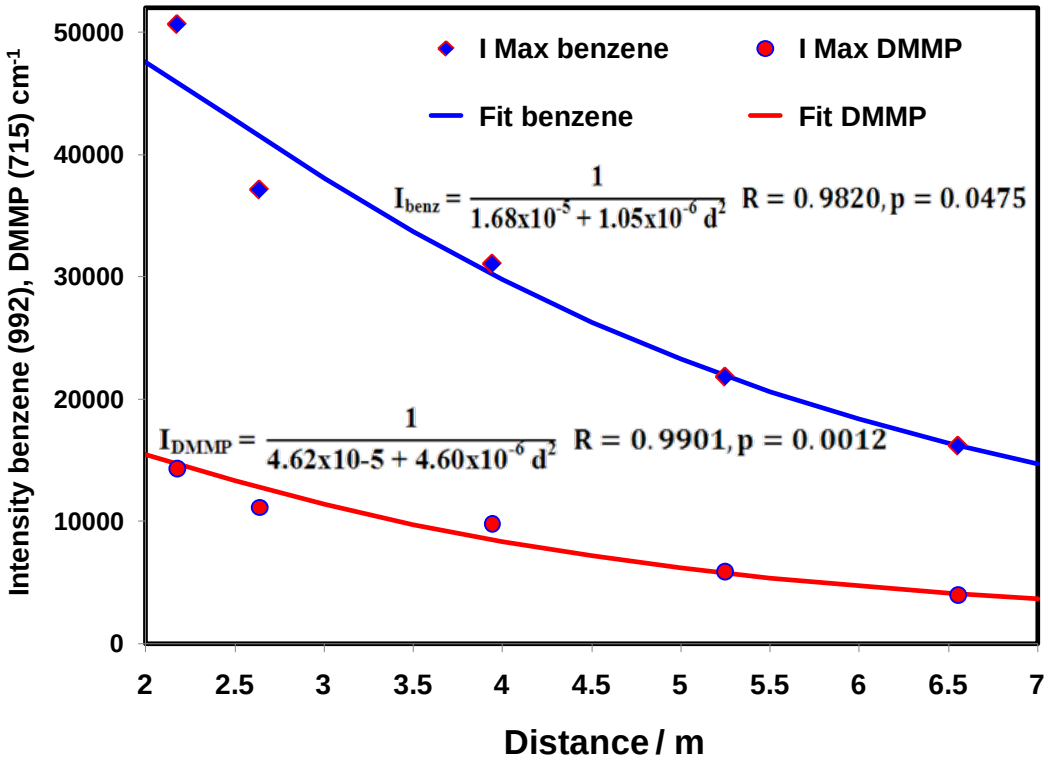

Figure 29. Dependence of Raman Shift signal (vibrational band intensities) with standoff distance for benzene and DMMP using the 363.8 nm excitation line from a UV-argon ion laser.

The current version of the CW laser remote spectroscopic system is probably less able to detect very long source-target distances (standoff distances) compared to pulsed laser systems

because of the higher energy densities in the beam axis of the pulsed systems. However, at close range, working as a near field detector, the CW standoff Raman detection system works equal or better than the pulsed system. The following two cases will provide experimental evidence for this supposition.

Remote Raman spectra were excited using uncollimated CW and pulsed laser beams. Laser power levels of CW lasers were 0.140 to 5.1 W. The calculated values for energy/area taking into account the laser beams spot size at the sample were 1.5 to 8.3 W/cm^2 (1.5 – 8.3 W/cm^3 energy densities for a sample vial 1-cm in diam). For the pulsed laser experiments, up to 1000 pulses of 200 mJ/pulse (6 ns, 10 Hz) were used, resulting in a maximum average power of 2.0 W. At a standoff distance of 6.6 m, the pulsed laser spot was an ellipse with a major semi-axis of 2.5 cm and minor semi-axis of 1.5 cm.

Table 3. Remote Raman spectroscopy systems laser beams characteristics.

λ (nm)	**Spot Diam. at 6.6 m (cm)**	**Area (cm^2)**	**Laser Power (Energy) (W / mJ)**	**Energy/Area (W/cm^2)**
532.0 (CW)	1.0	0.79	5.10	6.49
514.5	0.4	0.13	1.00	7.96
488.0	0.4	0.13	1.00	7.96
363.8	0.35	0.10	0.80	8.32
351.1	0.35	0.10	0.14	1.46
532.0 (pulsed)	2.5x1.5*	2.95	2.00 / 200	0.68

***** spot is elliptical in shape

This corresponds to an energy/area of 0.68 W/cm^2 (0.68 W/cm^3 in a 1-cm diam. vial) or roughly 47% of the minimum value for the steady-state detection system. Table 3. lists the relevant laser beam characteristics of the standoff system. In contrast, typical normal or spontaneous Raman measurements under the microscope use power density values on the order

of 12,500 W/cm^3 to excite the Raman Shift spectra of samples contained in capillary tubes (100 mW, 10x objective, 10 μm spot size in confocal mode, 8x10^{-6} cm^3 interrogation volume). This represents a 1,500 to 8,000-fold higher energy density value for the microscope experiments than the telescope-based CW Raman experiments

4.2.3 Relative Raman Scattering Cross Sections of CWAs

Raman scattering cross sections, $(d\sigma/d\Omega)_s$, of CWAS were calculated by performing intensity measurements and relating them according to the treatment of Christesen via Eq. 11 [30]:

$$\frac{\left(\frac{d\sigma}{d\Omega}\right)_s}{\left(\frac{d\sigma}{d\Omega}\right)_r} = \frac{A_s\, N_s\, n_s\, E_s}{A_r\, N_r\, n_r\, E_r} \qquad \textbf{(11)}$$

In the above equation, the subscripts s and r indicate the CWAS and reference values, respectively. A_s and A_r are the sample and reference integrated peak areas, which was measured from the spectra, and N_i is the number of molecules per unit volume, which was obtained from the sample and reference densities. The collection solid angle of the spectrometer is a function of the index of refraction of the liquid (n_i) and was accounted for by the ratio (n_s/n_r). E_i is an instrument efficiency factor that depends on the wavelength of the scattered light. If the sample and reference bands are close together (as they are typically chosen) the ratio E_s/E_r can be taken as 1. An additional factor would be necessary in Eq. 11 if either the sample or reference absorb at the laser wavelength [33].

Table 4. Relative differential Raman scattering cross sections.

Cross Sections ($x10^{-30}$ cm^2/sr/molecule)					
Exc. line (nm)	**benzene (992 cm^{-1})**	**cyclohexane (801 cm^{-1})**	**DMMP (715 cm^{-1})**	**2-CEES (700 cm^{-1})**	**2-BAET (1440 cm^{-1})**
532.0	13.4 [c]	3.6	3.7	2.8	2.7
488.0	32.5 [c]	9.06 [b]	18.0 [a]	15.1	20.3
363.8	328.4	105.6	58.0 [a]	21.4	10.3
351.1	160.0 [b]		17.2	5.4	3.3

Data adapted from: a ~ [25]; b ~ [26]; c ~ [27].

This method was applied to a comparison between the most prominent Raman band of the CWAS and the 992 cm^{-1} band of benzene and/or the 801 cm^{-1} band of cyclohexane. Benzene and cyclohexane were chosen as references (external primary standards). The cross-section data for the CWAS and reference compounds studied are shown in Table 4. These compounds are relatively weak Raman scatterers in comparison to the reference compounds. For this reason, the standoff detection of CWAS was an important instrument challenge, as suggested by Christesen [33].

4.2.4 Remote Raman Spectra of CWAs

The Remote Raman spectra of three CWASs: 2-BAET, 2-CEES and DMMP, are shown in Figure 30. All spectra were collected in the visible and NUV at a distance of 6.6 m from the collector telescope. The samples were detected using the strong blue line of the argon ion laser at 488.0 nm and NUV lines at 363.8 and 351.1 nm with 1 W laser power (at head) and a spectral acquisition time of 10 s. Raman peaks at 660 and 1440 cm^{-1} were tentatively assigned to C-S and C-N stretching vibrations, respectively, for the 2-BAET simulant (Fig. 25, top). A strong line appearing at about 700 cm^{-1} was tentatively assigned to C-Cl in 2-CEES (Fig. 30, center). Raman signals located about 660 and 750 cm^{-1} were attributed to the C-S and C-S-C of this simulant,

respectively. The peak at 715 cm^{-1} for DMMP (Fig. 25, bottom trace) was assigned to a P-C stretching mode.

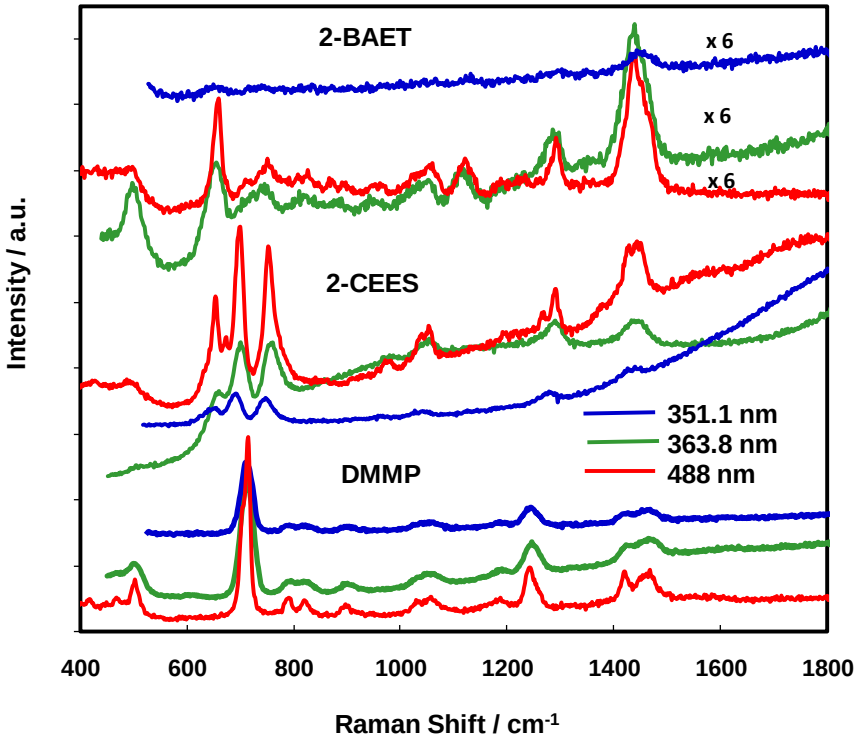

Figure 30. Remote Raman spectra of CWAS using excitation lines of 488.0, 363.8 and 351.1 nm at 6.6 m target-collector distance, 1 W laser power (at head) and one acquisition time of 10 s integration. Top: 2-(butylamino)-ethanethiol (2-BAET); center: 2-chloroethyl-ethyl sulfide (2-CEES); bottom : dimethylmethyl phosphonate (DMMP)

4.2.5 Remote Pulsed Raman Detection Measurements

Pulsed laser Standoff Raman spectra of cyclohexane and DMMP in the spectral range 500 - 3200 cm^{-1} are shown in Figures 31 and 32. The measurements were collected at distances of 35 m (DMMP) and 60, 90 and 141 m (cyclohexane) with gated detection using several 532 nm laser pulses (from 1 to 1000 shots) with 200 mJ per pulse. These experiments were

performed under “lights on” conditions. The most relevant spectroscopic information for both compounds was presented in the CW laser excitation section. Pulsed mode experiments were obtained using the ICCD camera, which was gated and synchronized with laser pulses to minimize interference from ambient light.

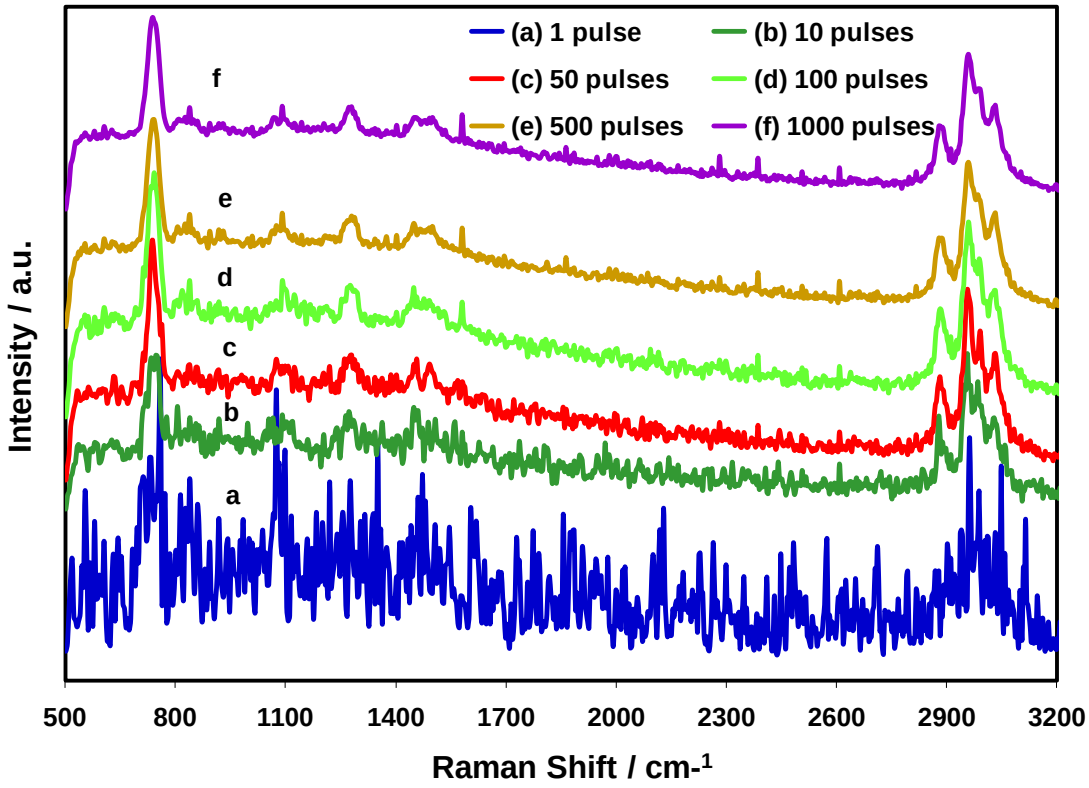

Figure 31. Remote Raman spectra of DMMP using a 532 nm pulsed laser excitation source at a distance of 35 m, measured with various laser shots in gated mode. Laser: 532 nm, 200 mJ/pulse, 10 Hz

The cyclohexane RRS spectra at 60 m and 90 m standoff distances were nearly identical. This similarity was the result of a size beam smaller that the target at both distances. However, the beam diameter at 141 m was significantly larger than the sample, which resulted in a reduced energy density and a lower scattering signal. However, even operating under these conditions, the cyclohexane spectrum at 141 m obtained with 1000 laser pulses had a good signal-to-noise

ratio (S/N = 450). The S/N value was determined by dividing the highest intensity Raman band of cyclohexane by the Root-Mean-Square (RMS) noise, calculated by taking a portion of the flattest region of the cyclohexane spectrum (1900-2100 cm^{-1}).

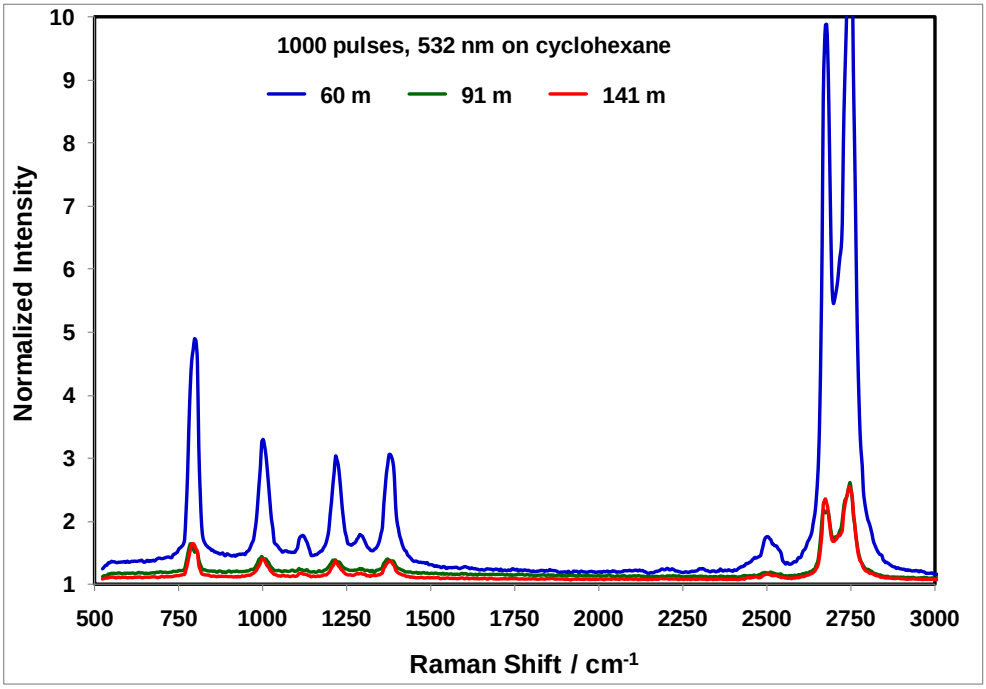

Figure 32. Remote Raman spectra of cyclohexane using a 532 nm pulse laser at standoff distances of 60, 90 and 141 m, measured with 1000 laser shots in gated mode. Laser: 532 nm, 200 mJ/pulse, 10 Hz; gate width 400 ns.

Both compounds can be detected with a single laser shot, but S/N became statistically significant by averaging the intensity collected after 10 laser shots, as can be seen in Figure 32. It is important to note the advantages of a pulsed laser system over CW systems for Raman detection at a distance. When operating in a gated detection mode, the background light signal and fluorescence signal are significantly reduced. Because the detector is acquiring for 400 ns, the fluorescence contributions that dominate at a longer time scale (~ μs) are minimized. One of the main disadvantages of the CW Remote Raman detection system is the necessity of operating

under low-illumination conditions. This problem can be readily circumvented by using a gated Intensified-Charge Coupled Device (I-CCD), UV-VIS-capable detector.

4.2.6 Remote CW Raman Quantification of DMMP in Water

An even more challenging application for the standoff Raman spectroscopy detection system was to perform quantification studies of a weak Raman scatterer mixed to less than 10% dilution with water. This task was undertaken using DMMP. In order to carry out the quantification experiments on DMMP, water, solutions of the analyte ranging from 1 to 50 % w/v were prepared and analyzed using CW RRS. For the quantification studies, peak areas of the strongest DMMP Raman signal located about 715 cm^{-1} were used (Figure 33).

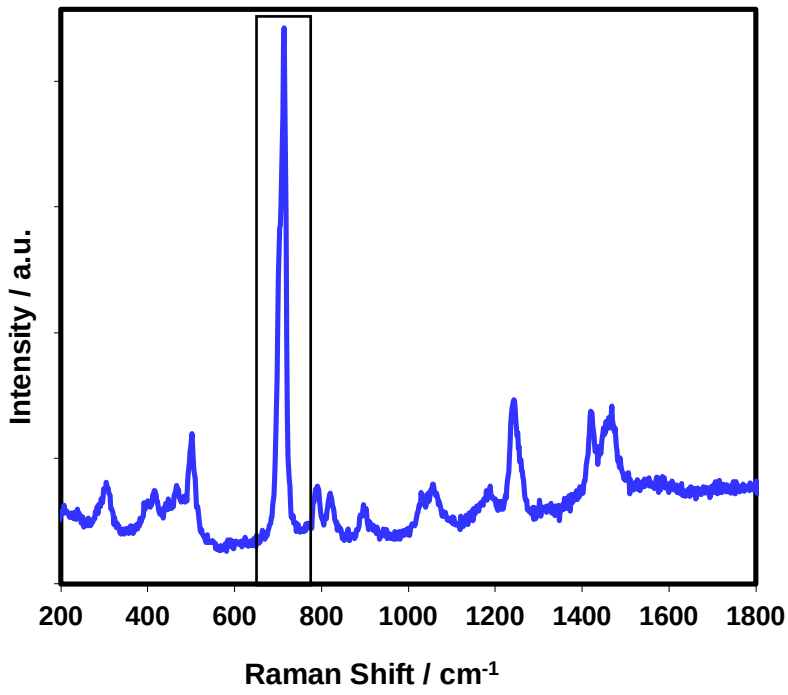

Figure 33. Raman signature of DMMP used for quantification in water solutions. The DMMP band located at 715 cm-1 was tentatively assigned to P-C symmetric stretching mode.

Figure 34 shows one of the calibration curves used for the quantification study of DMMP in aqueous solution. Calibrations were performed by three repetitive individual measurements for each sample of a concentration series ranging from 1 to 50 % w/v of DMMP in distilled water. For the measurements, the argon ion laser line at 488 nm was operated at a fixed laser power of 850 mW (at head), and an integration time of 15 s per acquisition was used. The error bars for each data point represent the calculated standard deviation derived from all measurements at each data point.

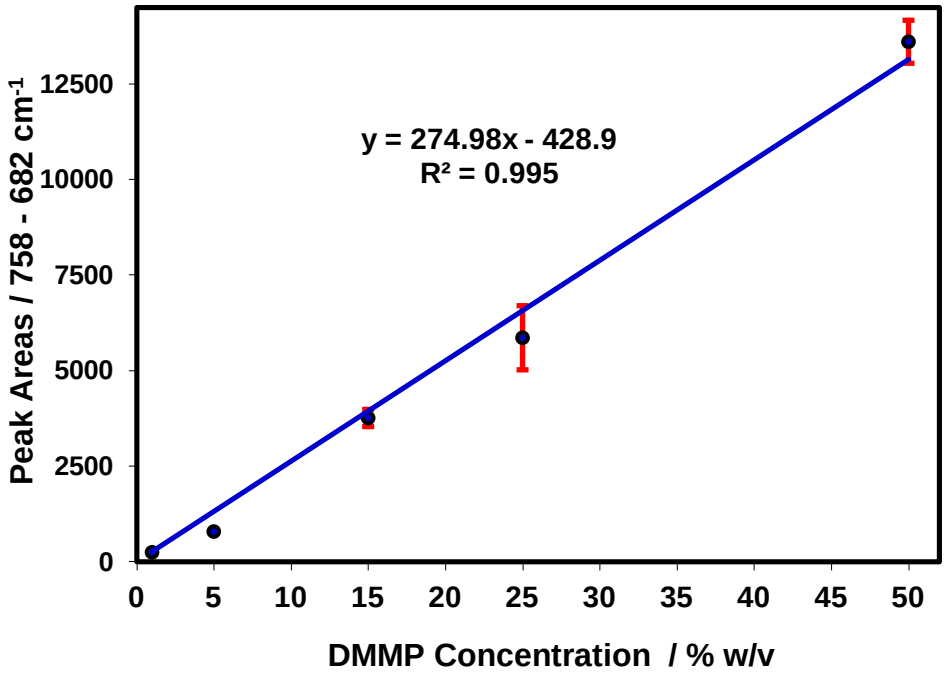

Figure 34. Quantification of DMMP in water by RRS measurements of DMMP solutions using a 488.0 nm excitation source, 850 mW laser power and a 15 s acquisition time at a standoff distance of 6.6 m.

The limit of detection (LOD) for this analyte was calculated according to IUPAC specifications using the following relationship (Eq. 12):

$$LOD = 3 (\sigma_b/m) \quad (12)$$

The IUPAC recommendation is to calculate the LOD values based on the "3σ" criterion: 3 times standard deviation of the peak-to-peak noise divided by the slope of the linear regression function [34]. The calculated LOD value was of 3 % w/v, which is remarkably low for a highly dilute solution of a weak Raman scatterer measured at 6.6 m from the excitation source using an approximate power/area of 6.8 W/cm^2.

4.3 Summary

Remote Raman systems have been designed, assembled and tested by coupling a Raman spectrometer with a reflective telescope using fiber optics. The CW RRS system employed 351.1, 363.8, 488.0, 514.5 and 532 nm continuous wave lasers as excitation sources. This prototype system was used in the detection of the chemical warfare agent simulants DMMP, 2-CEES and 2-BAET, and to detect the hazardous industrial solvents and reagents (TICs) benzene, toluene, chlorobenzene, carbon disulfide, carbon tetrachloride and cyclohexane. The operational range of the CW standoff system was tested up to 6.6 m in the laboratory with no background illumination. In addition, quantification studies of DMMP in water were carried out at a standoff distance of 6.6 m using the CW remote Raman detection system. Low limits of detection (LOD) values of 3% w/v were consistently obtained. The pulsed mode RRS system was based on a 532 nm, frequency doubled Nd:YAG laser in lieu the CW excitation lasers of allowed standoff detection experiments of DMMP at 35 m target-collector distances, from single shot to 1000 shots and also allowed detection of cyclohexane at 141 m standoff distance even in single shot mode. The Remote Raman Spectroscopy systems designed in this work should be useful for defense and security applications, for screening hazardous liquids in government installations, airports and seaports and in public installations to improve defense against terrorist attacks

5. Prediction and Discrimination of Explosives Hidden in Powder Mixtures by Remote Raman System

Explosives as well as illegal drugs can be strategically mixed with other compounds with similar chemical structure in order to confuse the authorities and make criminal or terroristic episodes. Therefore in this chapter focus on the detection and discrimination of dangerous compounds such as explosives (TNT and PETN) hidden in matrices non-explosives (4-nitrobenzoic acid and acetaminophen) with similar chemical structures were achieved in powder mixtures by remote Raman spectroscopy and chemometrics techniques

5.1 Reagents

The explosives reagents employed were 2,4,6-Trinitrotoluene (TNT), and Pentaerythritol tetranitrate (PETN), and the non-explosives compounds consisted of 4-nitrobenzoic acid toluene (4NBA) and acetaminophen (APAP). TNT was acquired from ChemService, Inc. (West Chester, PA) and the PETN was synthesized in the laboratory according to the method described by Urbanski [35]. The non-explosives were purchased from Aldrich-Sigma Chemical Co. (Milwaukee, WI).

5.2 Samples Preparation

Samples consisted of 24 powder mixtures prepared employing the compounds mentioned above and the compositions of the mixtures was ranging from 0 to 100% w/w, these values are tabulated in Table 5. Each component of the mixture was carefully weighed and mixed using an agate mortar ensuring homogeneity throughout the sample with a weight approximately of 300

mg. In order to design a robust detection model, the components of the mixture were strategically selected so that important Raman band of the explosives overlap with the band of non-explosives compounds, these Raman spectra can be appreciated in Figure 30.

5.3 Experimental setup

The Raman spectra of mixtures were collected employing a Remote Raman system (prototype III). This prototype was modified using Raman Explorer spectrograph with optical layout for 532nm (Headwall™ Photonics, Inc.) instead of the Andor spectrograph. Our remote Raman system consists of a MEADE ETX-125 Maksutov-Cassegrain telescope (125 mm clear aperture, 1900 mm focal length *f* /15). The reflecting collector was coupled to the Raman spectrometer with a non-imaging, 200 μm diameter optical fiber (model SR-OPT-8024, Andor Technology, Belfast, Northern Ireland). A frequency-doubled 532 nm Nd:YAG pulsed laser system (Quanta Ray INDI Series, Newport-Spectra Physics, Mountain View, CA) was used as the excitation source. The maximum energy/pulse of the laser at 532 nm was 25 mJ, and it operated at a repetition rate of 10 Hz. The pulse width was approximately 5-8 ns, and the beam divergence was less than 0.5 mrad. A gateable, intensified CCD detector (iStar™ ICCD camera, Model DH-720i-25F-03, Andor Technology, Belfast, Northern Ireland) was used as the photon detector. Andor Technology Solis™ software for spectroscopic, imaging and time-resolved studies was used for spectral data acquisition and processing from the intensified and gated CCD detector. Using this software, the data could be acquired in both imaging and spectroscopic modes.

5.4 Data collection

Each mixture was placed into a stainless steel sample holder of 0.6 cm in diameter where 30 ft·lb of pressure was applied to generate a tablet. Remote Raman spectra of mixtures were measured at a target to telescope standoff distance of 8 m, in the Raman Shift region 450-3000 cm^{-1} using an pulsed laser operating at 532 nm excitation line with a constant energy of 25mJ/pulse (at head) and 300 pulses were applied to achieve spectra with good Signal to Noise. A total of 10 spectra were collected for each mixture acquiring around 240 spectra in the specific Raman shift range.

5.5 Data analysis

The spectral data are subject to different inherent phenomenon during the acquisition process such as significant noises, baselines and others which can be undesirables factors, for that reason the performance of chemometrics analysis depend fundamentally on appropriate accomplishment of data preprocessing. Although different preprocessing methods such as vector normalization, multiple scattering correction (MSC), standard normal variate (SNV) first and second derivatives have been developed to improve a good quantification and discrimination analysis. These treatments can be illustrated in Figure 36(b). Partial least squares analysis (PLS) analysis were developed using the QUANT 2™ statistical tools provide by OPUS™ 6.0 software (Bruker Optics) to determinate the relationship between %w/w of component present in the mixture and Raman spectra. The 240 remote Raman spectra were randomly split into a two group, a first group with the 70% of the data for internal validation (calibration and cross validation) and external validation (test set) formed by the remaining 30% of the data. During PLS process the spectral outlier was detected by Mahalanobis distances method, where this

parameter is a measure of the similarity of the analyzed spectrum and the mean value of the all other [36]. Partial least squares discriminant analysis (PLS-DA) was developed in order to discriminate or classify between group such as explosives or non-explosives. This analysis was performed using PLS ToolBox™ 6.2 (Eigenvector, Wenatchee, WA) under Matlab™ platform.

5.6 Results and Discussion

Remote Raman spectra of the explosives (TNT and PETN), non-explosives (4-NBA acid and APAP) and a mixture of them are illustrated in Figure 35, these spectra were collected in the spectral region of 450-3000 cm^{-1} at a distance of 8 m from the telescope using a 532 nm pulse laser as excitation line.

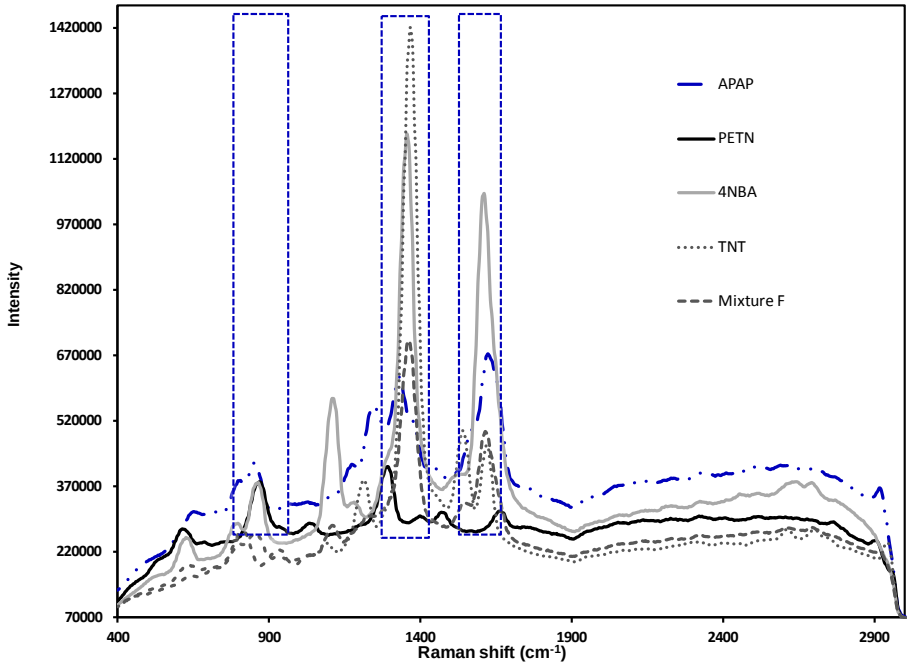

Figure 35.Remote Raman spectra of explosives (TNT and PETN), non-explosives (4-NBA and APAP) compounds and a mixture of them. These spectra were collected at 8 m from remote system employing 300 pulses of 532 nm laser

At first instance three spectral regions where clearly overlapping of vibrational bands of components are observed. The first Raman shift regions at 800 – 900 corresponding to NO2 scissoring mode, O-N stretching band, the second region from 1250 to 1400 cm-1 is relevant for NO2 symmetric stretching mode and the last spectral region localized around 1500 -1700 cm-1 are employed for NO2 asymmetric stretching mode, C=O stretching band[37-39].

Table 5. Composition (%w/w) of the compounds present in mixtures for the calibration models

	Component %w/w			
Mixture	**4NBA**	**PETN**	**TNT**	**APAP**
4NBA	100	0	0	0
PETN	0	100	0	0
TNT	0	0	100	0
APAP	0	0	0	100
Mix_A	5	15	20	60
Mix_B	25	15	20	40
Mix_C	5	40	20	35
Mix_D	25	40	20	15
Mix_E	5	15	35	45
Mix_F	25	15	35	25
Mix_G	5	40	35	20
Mix_H	25	40	35	0
Mix_I	15	27.5	27.5	30
Mix_J	28	35	0	37
Mix_K	26	29	0	45
Mix_L	43.3	0	18.3	38.3
Mix_M	45	0	15	40
Mix_N	59	0	0	41
Mix_O	70	10	5	15
Mix_P	88	3	0	9
Mix_Q	6.5	89.6	0.1	3.8
Mix_R	15	70	5	10
Mix_S	20	5	65	10
Mix_T	8	10	2	80

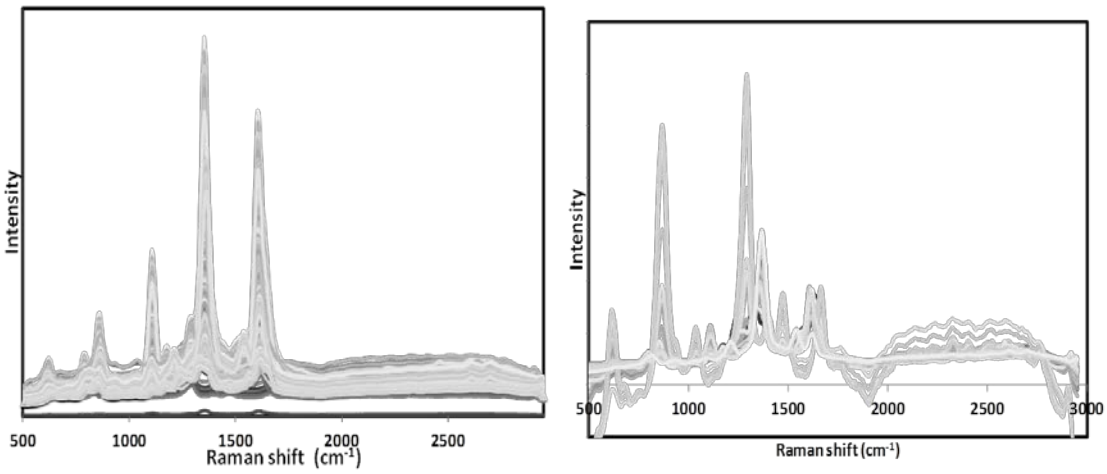

Figure 36. RR spectra of raw data (b) preprocessed data with MSC for all PLS models

Mixture of this type complicates the identification by simply visual spectroscopic analysis. Therefore chemometrics analysis emerges like powerful statistical tool for the quantification and discrimination process. To improve a good analysis was necessary to apply some pretreatment to the data before to chemometrics analysis. The results show that the normalization method such as multiplicative scattering correction was the most successful method for correcting background and this can be illustrated in Figure 36.

Where in 36 (a) corresponding to raw data and (b) shows the total spectra data after MSC preprocessing. The MSC method has been developed to eliminate or reduce the troubling effect of light scattering (small particles scatter light more than larger particles) and sometimes also called multiplicative signal correction, is one such technique which has shown to be very useful for improving multivariate linearity and prediction ability [40-42].

5.7 Chemometrics Analysis

All remote PLS models were built employing Leave-One-Out-Cross Validation to find the best correlation function between the Raman spectra and the concentrations (%w/w) of each

component present in the mixture and their Statistical accuracy was developed by the coefficient of determination (R^2), root mean square the standard error of cross validation (RMSECV) and the response of the calibration models versus test samples was evaluates by root mean square error of prediction (RMSEP). All quantification analysis for explosives and non-explosives were performed using MSC preprocessing data and different spectral regions where the variability in samples was more pronounced and the detailed results can be appreciated in the table 6 with 5% of the calibration data were detected as outliers in calibration and cross validation process and were removed from analysis.

In Figure 37 can be observed the PLS regression plots for explosives (TNT and PETN) and non-explosives (4NBA and APAP) compounds. Quantification analysis was achieved employing the different spectral regions for each compounds and these spectral range were tabulated in table 6. As shown in correlation plots, exist a good relationship between the true and predicted concentration (%w/w) with R^2 values of 99.53 and 98.63 for TNT and PETN respectively, and it can also be appreciated the good prediction of test set samples with value of RMSEP of 0.00165 and 0.0325% for corresponding explosives. For non-explosives quantification analysis whit higher R^2 (99.24 and 99.65 for 4NBA and APAP) and values and lower RMSECV were determinate, as well as explosives good RMSEP (0.0257 and 0.015% for 4NBA and APAP) were found as a criterion to judge the quality of method.

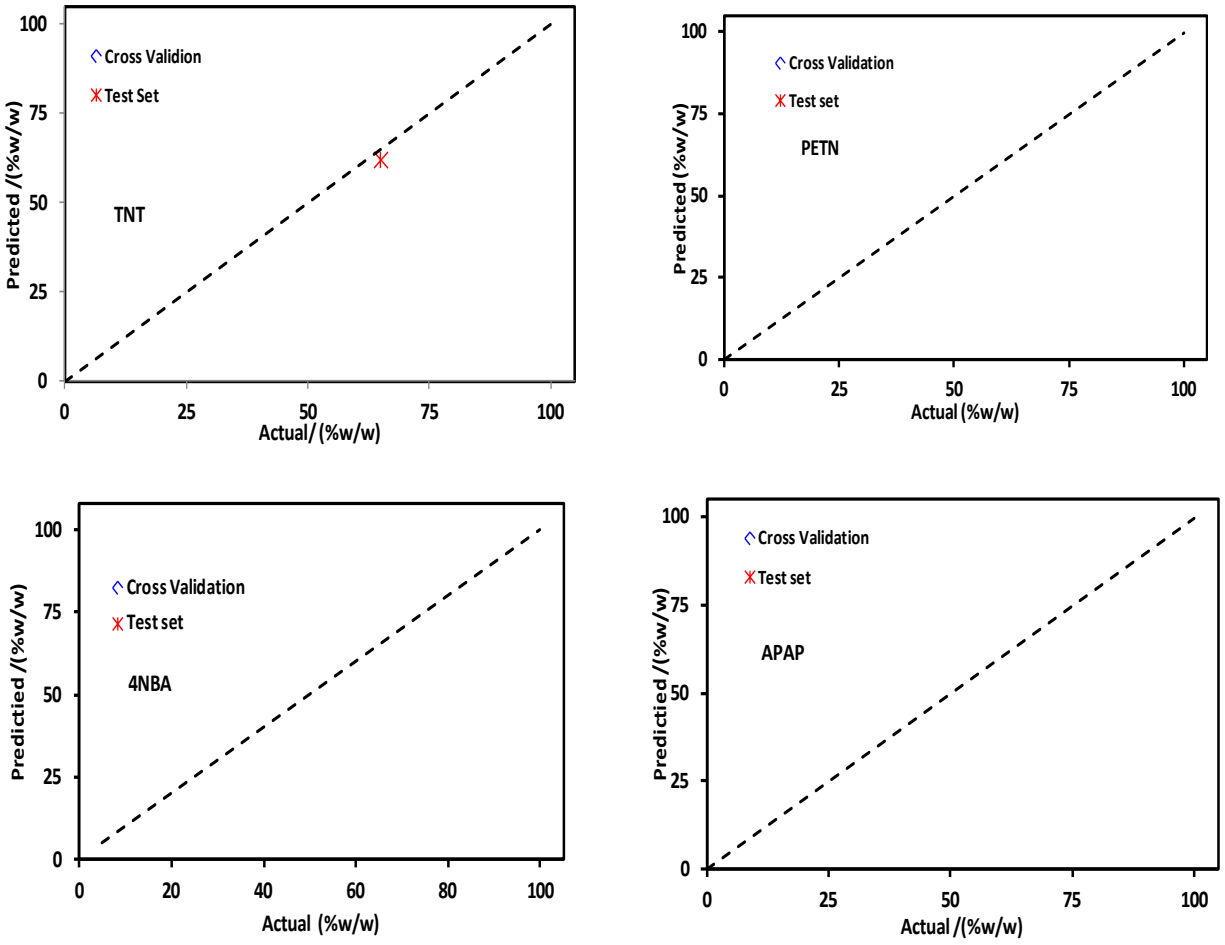

Figure 37. PLS plots for explosives (TNT and PETN) and non-explosives (4-NBA and APAP) compounds present in different mixtures.

The figures of merit such as multivariate detection and quantification limits (LOD, LOQ) for the optimal PLS models were calculated according to Felipe-Sotelo et al [43], with values below to 0.5% for all components. PLSDA was applied to establish the optimum separation of classes (explosives and non-explosives) using dummy variables 0 and 1. This analysis was achieved employing 20 remote spectra for explosive and 20 for non-explosives and assigning el value of 1 for explosives class and 0 for non-explosives class. the robustness of the model was tested by leave- one-out cross validation method and the performance of classification model

was tested by the sensitivity (number of samples predicted as in the class divided by number actually in the class) and specificity (number of samples predicted as not in the class divided by actual number not in the class) parameters.

Table 6. PLS summary for quantification of explosives and non-explosives at 8 m from the remote system employing 532 nm pulse laser as excitation line

	4NBA	**PETN**	**TNT**	**APAP**
Spectral Regions(cm-1)	2901-1968.7 1726-1477.4 1234-497.8	2901-2705.7 2217.3-1723.1 1234-740.8	2901-1723.1 1480-1231.8 989.1-497.8	2901.3-1231.8 989.1-740.5
Preprocessing Method	MSC	MSC	MSC	MSC
R^2 (CV)[a]	99.24	99.32	99.57	99.65
R^2 (P)	99.04	98.63	99.53	99.62
RMSECV	0.0234	0.0227	0.0157	0.0144
RMSEP	0.0257	0.0325	0.0165	0.015
Rank[b]	10	9	10	10
LOD (%w/w)	9	8	2.6	5
LOQ (%w/w)	27	26	17	16

CV[a] Cross-Validation.
Rank[b] correct numbers of factors to built PLS model.

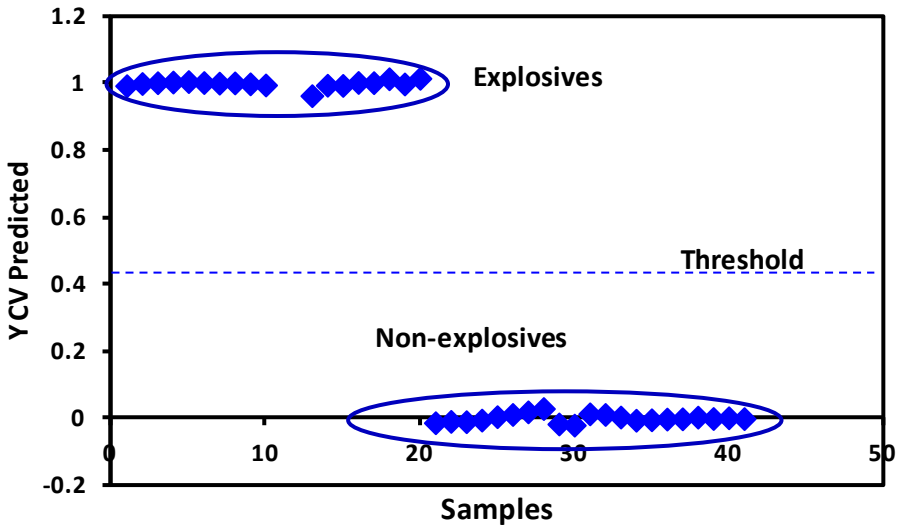

Figure 38. Cross-validated PLSDA plot for the discrimination of explosives and non-explosives compounds.

Figure 38, illustrates the cross-validated predicted classes versus samples, as shown in the PLSDA plot explosives class was located around 1 and non-explosives class around 0 and the dashed line indicates the threshold parameter. According to this analysis, that all cases were successfully classified employing only four latent variables with 100% of sensitivity and specifity and RMSEC of 0.008 which was considered statistically insignificant as a diagnostic threshold. The results obtained confirm that remote Raman spectroscopy employing chemometrics techniques become a powerful methodology for quantification and classification of dangerous compounds such as explosives.

5.8 Conclusion

Satisfactory results were found for the quantification of explosives and non-explosives with good values of R^2, RMSECV. Reliable predictions and discrimination with100% de sensitivity and specifity obtained by remote sensing based on Raman spectroscopy at remote distance 8 m employing 532 nm laser as excitation source. Remote Raman system using the appropriate chemometrics tools such as PLS and PLSDA promises to be a reliable technique for verdict of the existence of high energetic material such as explosives deliberately hidden in matrices with similar chemical structure. The Remote Raman Spectroscopy systems designed in this work should be useful for defense and security applications, for screening hazardous liquids in government installations, seaports and in public installations to improve defense against terrorist attacks

REFERENCES

1. Sun Y, Ong KY, Detection Technologies for Chemical Warfare Agents and Toxic Vapors; Taylor & Francis Group, 2005.
2. Farquharson S, Gift A, Maksymiuk P, Inscore FSurface-enhanced Raman spectra of VX and its hydrolysis products. *Appl. Spec*. **2005**, 59, 654-659.
3. Smentkowski VS, Hagans P, Yates JT. Study of the Catalytic Destruction of Dimethyl Methylphosphonate Oxidation over Mo(ll0). *Phys. Chem*. **1998**. 92, 6351-6357.
4. Marrs TC, Maynard R L, Sidell FR. Chemical Warfare Agents: Toxicology and Treatment, John Wiley & Sons Ltd., London, UK, **1996.**
5. Steinfeld JI, Wormhoudt . *Annu Rev. Phys. Chem*. **1998**, 49, 203.
6. Hirschfeld T. Range Independence of Signal in Variable Focus Remote Raman Spectrometry. *Appl. Opt*. **1974**, *13*, 1435.
7. Angel SM, Kulp TJ, Vess TM. *Appl. Spec*.**1992**, *46*,1085
8. Wu M, Ray M, Fung KH, Ruckman MW, Harder D, Sedlacek III A. Stand-off detection of chemicals by UV Raman spectroscopy. *Appl. Spectrosc.* **2000**, *54,* 800-806.
9. Sedlacek III , AJ, Ray MD, Higdon NS, Richter DA. Short-range noncontact detection of surface contamination using Raman lidar *Proc. SPIE*. **2001**, *95,* 4577.
10. Sharma SK, Angel SM, Ghosh M, Hubble HW, Lucey PG. A remote pulsed-laser Raman spectroscopy system for mineral analysis on planetary surfaces to 66 meters. *Appl. Spectrosc* **2002**, *56,* 699-705.
11. Thomson G, Batchelder D. *Rev. Sci. Instrum.* **2002**, *73:* 4326.

12. Sharma SK, Lucey PG, Ghosh M, Hubble HW, Horton K. A Stand-off Raman Spectroscopic Detection of Minerals on Planetary Surfaces. *Spectrochim. Acta A.***2003**, *59,*2391-2407
13. Sharma SK, Anupam KM, Bhavna S. Portable remote Raman system for monitoring hydrocarbon, gas hydrates and explosives in the environment. *Spectrochim. Acta, Part A.* **2005**, *61,* 2404-2412.
14. Pacheco-Londono LC, Ortiz-Rivera W, Primera-Pedrozo O. M., Hernandez-Rivera SP Vibrational spectroscopy standoff of explosives. *Anal. Bioanal. Chem*. **2009**, 395,323–335.
15. Ortiz-Rivera W, Pacheco-Londono LC, Hernandez-Rivera, S. P. Remote continuous wave and pulsed laser Raman detection of chemical warfare agents stimulants and toxic industrial compounds. Sens Imaging. **2010**, 11,131-145.
16. Ramirez ML, Ortiz-Rivera W, Pacheco-Londoño LC, Hernandez-Rivera, S. P. Remote detection of hazardous liquids concealed in glass and plastic containers. IEEE J. Sensors. **2010**,10, 693-699.
17. Miller FA, Kauffman GB, C.V. Raman and the discovery of Raman effect. *J.Chem.Educ.***1989**, 66,795-801.
18. Tobias RS, Raman spectroscopy in inorganic chemistry. *J.Chem.Educ*. **1967**, 44, 2-8.
19. Misra A, Sharma SK, Lucey PG. Remote Raman Spectroscopy detection of minerals and or organics under illuminated conditions from a distance of 10 m using a single 532 nm laser pulse. *Appl. Spectrosc.* **2006**, *60,* 223-228.
20. Carter J C, Angel SM, Lawrence-Snyder M S, caffidi J, Whipple RE, Reynolds JG Standoff detection of high explosive materials at 50 meters in ambient light conditions using a small Raman instrument. *Appl. Spectrosc*. **2005**,*59,*769–775.

21. Pettersson, A, Johansson, I, Wallin, S, Nordberg, M, Östmark, Near Real-Time Standoff Detection of Explosives in Realistic Outdoor Environment a at 55m Distance *Propellants Explos., Pyrotech.* **2009,** 34, 297-306.
22. Angel, S. M; Gomer, N. R.; Sharma, S. K.; McKay, C. **2012,** 66, 137-150.
23. Karpowicz RJ, Brill TB. Comparison of the molecular structure of hexahydro-1,3,5-trinitro-s-triazine in the vapor, solution and solid phases. *J. Phys. Chem.***1984**, *88*, 348-352.
24. Shimanouchi, T. *Tables of Molecular Vibrational Frequencies Consolidated*. Nat. Stand.Ref.Data Ser., Nat. Bur.Stand.(U.S), **1972**, 39, 164.
25. Lin-Vien, D. Colthup, N. B. Fateley, W. B. & Graselli, J. G. *The Handbook of Infrared and Raman Characteristic Frequencies of Organic Molecules*, Boston, MA, **1991**.
26. Schrader, B. *Infrared and Raman spectroscopy: Methods and applications*. New York, NY, 1995.
27. McCreery, R. L. *Raman Spectroscopy for Chemical Analysis*. New York, NY: Wiley-Interscience, 2000.
28. Evans J C, Bernstein HJ. The effect of Intermolecular interaction on Raman spectrum of carbon disulphide. *Can. J. Chem.***1956**, 54, 1127-1133.
29. Wakabayashi, K., Matsumura, T., Nakayama, Y., Koshi, M. Temporal change of Raman spectra of carbon tetrachloride under laser-driven shock compression. *AIP Conference Proceedings*. **2007**, 955, Issue 1, 1267-1270.
30. Crain J, Poon WC, Cairns-Smith A, Hatton PD. High-pressure Raman spectroscopic study of cyclohexane C_6H_{12} and C_6D_{12}. *J. Phys. Chem*. **1992**, 96,8168-8173.

31. Pacheco-Londono LC, Ortiz-Rivera W, Primera-Pedrozo OM, Hernandez-Rivera SP. Vibrational spectroscopy standoff of explosives *Anal. Bioanal. Chem*. **2009**, *39*,323-335
32. Sharma SK, New trends in telescopic remote Raman spectroscopic instrumentation. *Spectrochim. Acta A*, **2007**, 68, 1008-1022.
33. Christesen SD. Raman cross sections of chemical agents and simulants. *Appl. Spectrosc*. **1988**, *42*, 318-321.
34. Mocak J, Bond AM, Mitchell S, Scollary GA. statistical overview of standard (IUPAC and ACS) and new procedures for determining the Limits of de tection and quantification: application to voltammetric and stripping techniques *Pure Appl. Chem.* **1997**, *69*, 297-328.
35. Urbanski T Chemistry and technology of explosives, Macmillan Company, New York,1964.
36. De Maesschalck R, Jouan-Rimbaud D, Massart DL *Chemom Intell Lab Syst*. **2000**, 50,1-18.
37. Gruzdkov YA, Gupta YM *J. Phys Chem. A* ,**2001**,105, 6197-6202.
38. Lewis IR, Daniel NW, Griffiths PR . *Appl. Spectrosc*. **1997**, 51,1854-1868.
39. Pestaner JP, Mullick FG, Centeno JA *J Forensic Sci.* **1996**, *41*,1060-1063.
40. Geladi P, McDougel D, Martens H. *Appl Spectrosc,* **1985**, 39,491-500.
41. Barnes RJ, Dhanoa MS, Lister SJ. *Appl Spectrosc.* **1989**, 43,772-777.
42. Chen JY, Iyo C, Terada F, Kawano S*J. Near Infrared Spectrosc.* **2002**, 10,301-307.
43. Felipe-Sotelo M., Cal-Prieto MJ, Ferre´ J, Boque R , Andrade JM, Carlosena A, J. Anal. At. Spectrom. **2006**, 21: 61-68.